Received: 22 April 2020 | Revised: 24 August 2020 | Accepted: 25 August 2020

DOI: 10.1111/jne.12904

ORIGINAL ARTICLE

Journal of Neuroendocrinology WILEY

Dopamine-induced interactions of female mouse hypothalamic proteins with progestin receptor-A in the absence of hormone

Kalpana D. Acharya[1] | Sabin A. Nettles[1] | Cheryl F. Lichti[2] | Katherine Warre-Cornish[3,4] | Lucia Dutan Polit[3,4] | Deepak P. Srivastava[3,4] | Larry Denner[5] | Marc J. Tetel[1]

[1]Neuroscience Department, Wellesley College, Wellesley, MA, USA

[2]Department of Pathology and Immunology, Washington University School of Medicine, St Louis, MO, USA

[3]Department of Basic and Clinical Neuroscience, The Maurice Wohl Clinical Neuroscience Institute, Institute of Psychiatry Psychology and Neuroscience, King's College London, London, UK

[4]MRC Centre for Neurodevelopmental Disorders, King's College London, London, UK

[5]Department of Internal Medicine, University of Texas Medical Branch, Galveston, TX, USA

Correspondence
Kalpana D. Acharya, Neuroscience Department, Wellesley College, 106 Central Street, Wellesley, MA 02481, USA.
Email: kacharya@wellesley.edu

Funding information
NIH Clinical Center, Grant/Award Number: 5U24DK076169-13 (RM) Subaward # 30835-64 (KDA) and R01 DK61935 (MJT); European Union's Seventh Framework Programme for research, Grant/Award Number: 603016 (DPS)

Abstract

Neural progestin receptors (PR) function in reproduction, neural development, neuroprotection, learning, memory and the anxiety response. In the absence of progestins, PR can be activated by dopamine (DA) in the rodent hypothalamus to elicit female sexual behaviour. The present study investigated mechanisms of DA activation of PR by testing the hypothesis that proteins from DA-treated hypothalami interact with PR in the absence of progestins. Ovariectomised, oestradiol-primed mice were infused with a D1-receptor agonist, SKF38393 (SKF), into the third ventricle 30 minutes prior to death. Proteins from SKF-treated hypothalami were pulled-down with glutathione *S*-transferase-tagged mouse PR-A or PR-B and the interactomes were analysed by mass spectrometry. The largest functional group to interact with PR-A in a DA-dependent manner was synaptic proteins. To test the hypothesis that DA activation of PR regulates synaptic proteins, we developed oestradiol-induced PR-expressing hypothalamic-like neurones derived from human-induced pluripotent stem cells (hiPSCs). Similar to progesterone (P4), SKF treatment of hiPSCs increased synapsin1/2 expression. This SKF-dependent effect was blocked by the PR antagonist RU486, suggesting that PR are necessary for this DA-induced increase. The second largest DA-dependent PR-A protein interactome comprised metabolic regulators involved in glucose metabolism, lipid synthesis and mitochondrial energy production. Interestingly, hypothalamic proteins interacted with PR-A, but not PR-B, in an SKF-dependent manner, suggesting that DA promotes the interaction of multiple hypothalamic proteins with PR-A. These in vivo and in vitro results indicate novel mechanisms by which DA can differentially activate PR isoforms in the absence of P4 and provide a better understanding of ligand-independent PR activation in reproductive, metabolic and mental health disorders in women.

KEYWORDS
energy homeostasis, induced pluripotent stem cells, metabolism, progesterone, synapse

1 | INTRODUCTION

Neural progestin receptors (PR) are important regulators of neuroprotection,[1-5] learning and memory,[6-8] anxiety and stress response,[9-12] energy homeostasis, and reproduction.[13-16] Many of these effects are mediated by PR expressed in the hypothalamus.[14,17-19] In rodents and humans, PR are expressed as two isoforms, comprising an N-terminally truncated PR-A and a full-length PR-B,[18,20-22] which are transcribed from alternate transcription start sites of the same *pgr* gene.[20,23] Although both PR isoforms share a C-terminal ligand binding domain, a DNA binding domain and two transactivation domains, differences between the two isoforms are contributed by a PR-B-specific transactivation domain and a PR-A-specific inhibitory region.[18,20,23-26] These structural differences contribute to the differential transcriptional activity of PR-A and PR-B in vitro and in vivo.[27-32] For example, using PR isoform-specific knockout mice, Mani et al. [33] have shown that PR-A is the primary mediator of female reproductive behaviour, although both PR isoforms are essential for the full behavioural response. These dominant effects of PR-A on behaviour may be partially a result of differential expression of the isoforms in the hypothalamus.[17] Similarly, the PR isoforms have distinct functions in peripheral tissues, such that PR-A is primarily responsible for follicular maturation and embryo implantation, whereas PR-B is the major mediator of mammary gland growth and proliferation.[34,35]

As with other steroid receptors, PR are transcription factors that directly bind to DNA and initiate gene transcription. This PR-mediated transcription is enhanced by interaction with coregulator proteins, including steroid receptor coactivator-1 (SRC-1), SRC-2 and CBP (CREB-binding protein), which are necessary for PR-dependent gene expression and female reproductive behaviour.[36-38] Recently, using proteomics-based approaches, we identified a repertoire of hypothalamic proteins, including synaptic proteins, kinases, and transcriptional, translational and metabolic regulators, that associate with PR in a hormone- and isoform-dependent manner.[16] In addition, we found that progesterone (P4) enhanced synaptic density by increasing synapsin (SYN)1-positive synapses in rat primary cortical neurones, suggesting that progestins function in synaptic plasticity.[16] In support, PR are expressed in extra-nuclear compartments, including synapses,[39,40] and alter dendritic spine densities in the hippocampus,[41,42] cortex[43,44] and hypothalamus.[45] These findings provide insights into the multiple pathways and novel functions mediated by progestin-activated PR in brain.

Although it is well established that PR acts as a ligand-induced transcription factor to elicit gradual and long-lasting changes,[18,38,46] PR-A and PR-B can also be activated in the absence of hormone by the neurotransmitter dopamine (DA).[14,47-49] DA activation of PR in rat and mouse hypothalamus acutely induces female reproductive behaviour in the absence of P4.[33,50] However, there is a lack of understanding of the mechanisms for this DA-dependent PR activation in the hypothalamus and the induction of female reproductive behaviour. One possible mechanism for this activation of hypothalamic PR is a DA-induced cascade resulting in the phosphorylation of hypothalamic proteins that interact with PR in the absence of P4. These DA-induced interactions of hypothalamic proteins with PR could elicit changes in receptor function, including transcription, thus modifying behaviour.[16,51-53] Therefore, in the present study, using pull-down assays combined with mass spectrometry (MS), we tested the hypothesis that proteins from female mouse hypothalamus treated with a D1 receptor (D1R) agonist would interact with PR in the absence of progestins. Following identification of a large set of synaptic proteins, we developed gonadotrophin-releasing hormone (GnRH)-positive hypothalamic-like neurones derived from human-induced pluripotent stem cells (hiPSCs) that express 17β-oestradiol (E_2)-induced PR to test the hypothesis that DA activation of PR contributes to an increase in synaptic protein expression.

2 | MATERIALS AND METHODS

2.1 | Animals

Female C57/BL6 mice were bred in the Wellesley College Animal Facility and group-housed (3-6 per cage) prior to surgery. A 12:12-hour light/dark cycle was maintained and food and water were provided ad lib. All animal procedures were approved by the Institutional Animal Care and Use Committee of Wellesley College and were conducted in accordance with the National Institutes of Health Guide for the Care and Use of Laboratory Animals guidelines.

2.2 | Ovariectomy and stereotaxic surgery

Eight-week old C57/BL6 mice (n = 18) were bilaterally ovariectomised under 1.5% isoflurane. Stereotaxic surgery was performed to implant cannula (22-gauge, #8IC313GS5SPC; Plastics One, Roanoke, VA, USA) aimed at the third ventricle in the midline, anteroposterior: −1.5 mm from bregma, dorsoventral −5 mm, as described previously.[54] A dummy cannula was inserted into the guide cannula to keep the tract intact until drug infusion. Mice were individually housed following stereotaxic surgery to prevent cannula displacement by cagemates and to recover from surgery for one week. Then, all mice were injected s.c. with oestradiol benzoate (EB; 1 μg in sesame oil, #E-8515; Sigma-Aldrich, St Louis, MO, USA) to induce PR expression in the hypothalamus.[17] Forty-eight hours after EB administration, mice were infused with a D1R agonist, SKF 38393 (SKF; #D047; Sigma-Aldrich) or vehicle (Veh, 0.9% sterile saline), through the injector cannula (28 gauge) into the third ventricle. SKF (100 ng in 2 μL of 0.9% sterile saline) was infused at a rate of 1 μL min^{-1} using a 22-gauge Hamilton syringe attached to a stereotaxic instrument (Stoelting, Wood Dale, IL, USA).[54] Thirty minutes after the infusion, mice were killed by asphyxiation under CO_2 (Figure 1). This dose and time frame for SKF treatment has been previously shown to be sufficient for the PR-dependent expression of sexual receptivity, selectively through D1R activation.[33,54-56]

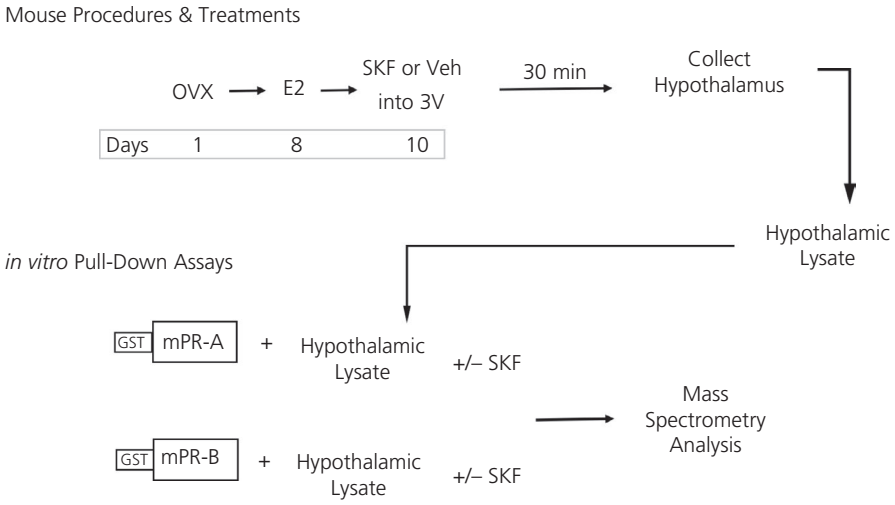

FIGURE 1 Experimental outline. Timeline of procedures and treatments of mice prior to collection of the hypothalamic tissue and in vitro protein-protein pull-down assays with glutathione *S*-transferase (GST)-tagged mouse progestin receptors (PR) and hypothalamic lysates treated with (+) or without (–) SKF. OVX, ovariectomy; 3V, third ventricle; mPR, mouse progestin receptor

2.3 | Tissue collection and protein extraction

Hypothalamic tissue was dissected using coordinates from the mouse brain atlas[57], immediately frozen on dry ice, and stored at −80°C until protein extraction. Hypothalami from nine mice were pooled to generate each sample. Tissue was added in a tube with Lysing Matrix D (#6913; MP Bio, Santa Ana, CA, USA) and lysis buffer (10 mmol L^{-1} Tris, 10% glycerol, 400 mmol L^{-1} NaCl, 1 mmol L^{-1} dithiothreitol (DTT) with ethylenediamine tetraacetic acid (EDTA) (1 mmol L^{-1}, pH 7.4), phosphatase inhibitors (50 mmol L^{-1} NaF and 1 mmol L^{-1} Na_3VO_4, and protease inhibitors (dilution 1:10; #P2714; Sigma-Aldrich). The tissue/lysis buffer was added at a ratio of 2:1. The mixture was homogenised at 4 m s^{-1} at four 5-second cycles using Fast Prep 24 (MP Bio), with a 5-second incubation on ice between every cycle to avoid sample degradation from heating. Lysates were incubated on ice for 30 minutes followed by centrifugation at 13 200 *g* for 30 minutes at 4°C. Supernatants containing proteins were stored at −80°C.

2.4 | Glutathione *S*-transferase (GST)-tagged mouse PRs

Mouse PR-A and PR-B complementary DNAs (cDNAs) were cloned into the CMV-based mammalian cell expression plasmid pcDNAI (Invitrogen, Carlsbad, CA, USA), as described previously.[16] The DNA construct sequences were verified from the start of the GST to the end of the mouse PR (Genewiz, South Plainfield, NJ, USA). The recombinant proteins containing full-length mouse PR-A or PR-B fused to a GST tag were expressed in *Spodoptera frugiperda* (Sf9; RRID:CVCL_0549) insect cells at the Baculovirus/Monoclonal Antibody Facility of the Baylor College of Medicine as described previously.[16,58] Insect cell cultures for GST-PR-A or GST-PR-B were grown in the absence of PR ligand. The Sf9 cell pellets containing PR were homogenised in buffer containing 10 mmol L^{-1} Tris, 10% glycerol, 400 mmol L^{-1} NaCl, 1 mmol L^{-1} and DTT, 1 mmol L^{-1} EDTA (pH 7.4) with protease inhibitors (dilution 1:10; #P2714; Sigma-Aldrich). Lysates were incubated on ice for 30 minutes, followed by centrifugation at 106 000 *g* for 30 minutes at 4°C. Supernatants containing receptors were stored at − 80°C.

2.5 | GST-PR pull-down assays

Pull-down assays were done using GST-PR-A or GST-PR-B with either SKF-, or Veh- treated hypothalamic lysates (Figure 1), as described previously.[16] In brief, glutathione sepharose 4B packed resin (50 µL, 0.05 mg mL^{-1}; Amersham Biosciences, Little Chalfont, UK) was pretreated with ovalbumin (1 mg mL^{-1}; Thermo Fisher Scientific, Waltham, MA, USA) for 15 minutes in siliconised centrifuge tubes on an end-over-end rotator at 4°C. Resin was rinsed three times with TG buffer (20 mmol L^{-1} Tris-HCl, 10% glycerol) containing 1 mol L^{-1} urea and 100 mmol L^{-1} NaCl (TG-NaCl-U, pH 8.0). Unliganded GST-PR-A or GST-PR-B, in equal amounts, were suspended in TG buffer with 1 mol L^{-1} urea (TG-U, pH 8.0) and were incubated with resin on a rotator at 4°C for 1 hour The immobilised GST-PR in resin was washed four times with TG-NaCl-U (with gradient urea concentrations of 1, 0.5, 0.25 and 0 mol L^{-1}). Equal amounts of pooled hypothalamic homogenates from each treatment condition were added to immobilised GST-PR and incubated on a rotator for 1 hour at 4°C, followed by four washes with TG-NaCl (without urea). Proteins bound to GST-PR resin were eluted by incubating in 250 mmol L^{-1} glutathione elution buffer (50 mmol L^{-1} Tris-HCl, pH 8.0) at 4°C for 10 minutes. Any remaining proteins in the resin were eluted by boiling for 5 minutes in 2 × Laemelli sample buffer (Bio-Rad, Hercules, CA, USA) with 35 mmol L^{-1} DTT (Sigma-Aldrich), which was used for confirmation of representative MS results by western analysis.

2.6 | Nano-liquid chromatography (LC) MS/MS analysis

Tryptic peptides from pull-down assays with unliganded GST-PR-A or GST-PR-B, were prepared as described previously.[16] Samples were block randomised and analysed in triplicates [59] and peptide

mixtures were analysed by nanoflow LC-MS/MS using a nano-LC chromatography system (UltiMate 3000 RSLCnano; Dionex, Sunnyvale, CA, USA), coupled on-line to a Thermo Orbitrap Fusion mass spectrometer (Thermo Fisher Scientific) through a nanospray ion source (Thermo Fisher Scientific). A trap and elute method was used with a C18 PepMap100 trap column (300 μm × 5 mm, 5 μm particle size; Thermo Fisher Scientific). The analytical column was an Acclaim PepMap 100 (75 μm × 25 cm; Thermo Fisher Scientific). After equilibrating the column in 98% solvent A (0.1% formic acid in water) and 2% solvent B (0.1% formic acid in acetonitrile, the samples (1 μL in solvent A) were injected onto the trap column and subsequently eluted (400 nL min^{-1}) by gradient elution onto the C18 column: isocratic at 2% B, 0-5 minutes; 2% to 45% B, 2-37 minutes; 45% to 90% B, 37-40 minutes; isocratic at 90% B, 40-45 minutes; 90% to 2%, 45-47 minutes; and isocratic at 2% B, 47-60 minutes.

All LC-MS/MS data were acquired using XCALIBUR, version 2.1.0 (Thermo Fisher Scientific) in positive ion mode using a top speed data-dependent acquisition method with a 3-second cycle time. The survey scans (*m/z* 370-1570) were acquired in the Orbitrap at 120 000 resolution (at *m/z* 400) in profile mode, with a maximum injection time of 56 msec and an AGC target of 600 000 ions. The S-lens RF level was set to 60. Isolation was performed in the quadrupole with a 1.6-Da isolation window and higher-energy collisional MS/MS acquisition was performed in centroid mode using rapid scan rate with detection in the ion trap, with the settings: collision energy = 32%; maximum injection time 56 msec; AGC target 200 000 ions. Monoisotopic precursor selection and charge state filtering were on, with charge states 2-6 included. Dynamic exclusion was used to remove selected precursor ions, with a ± 10 ppm mass tolerance, for 15 seconds after acquisition of one MS/MS spectrum.

2.7 | Proteomic data analysis

Tandem mass spectra were extracted and charge state deconvoluted by PROTEOME DISCOVERER, version 1.4.1.14 (Thermo Fisher Scientific). Deisotoping was not performed. All MS spectra were searched against a UniProt murine database (version 08-11-2014) using SEQUEST[60] Searches were performed with a parent ion tolerance of 5 ppm and a fragment ion tolerance of 0.60 Da. Trypsin was specified as the enzyme, allowing for two missed cleavages, fixed modification of carbamidomethyl (C) and variable modifications of oxidation (M). False discovery rate (FDR) estimation was allowed where peptide-spectrum matches above an FDR of 1% were used to generate a spectral library for the quantitative analysis. Data files for each pair of samples were imported into SKYLINE[61] for label-free quantitative analysis.[62] Following manual verification of all peaks, triplicate peptide intensities were used to calculate fold changes. The cleaned data were analysed using Student's *t* test to determine the effect of SKF within each PR subtype. Proteins from SKF-treated brains that had a ≥2-fold association with GST-PR, compared to the Veh-treated brains, with $P < 0.05$, were considered to show an SKF-dependent interaction.

2.7.1 | Ingenuity pathway analysis of the PR interactome

Proteins were classified into functional groups based on their primary functions in the UniProt database (http://uniprot.org). Of the identified proteins, those that belonged to the two largest functional groups, (i) synaptic proteins and (ii) regulators of cellular and energy metabolism, were interactively modelled using IPA (Ingenuity Analysis Application; Qiagen, Valnecia, CA, USA). The relationships depicted in the generated pathway are based on the literature-based interconnectivity data stored in the Ingenuity Knowledge Base Repository (Qiagen). In the network pathway, the types of biological relationships between two proteins are represented using different types of lines.

2.8 | Western blot analysis

Western blot analysis was performed as described previously[16] to qualitatively confirm the MS results for proteins involved in synaptic plasticity (SYN2 and protein phosphatase 1 regulatory subunit 1B, DARPP-32) and metabolism (creatine kinase B). SYN2 and creatine kinase B were chosen because they were identified to interact with liganded PR in our earlier study,[16] whereas DARPP-32 was shown to be an obligatory mediator of dopamine (DA)-induced female reproductive behaviour.[55] Pull-down samples were probed with the following primary antibodies: SYN2, targeted against domains A and B (mouse monoclonal, 0.3μg mL^{-1}, #mabn1573, Millipore, Billerica, MA, USA; RRID:AB_2828028); DARPP-32, targeted against the N-terminus (amino acids 1-100; rabbit monoclonal; dilution 1:100, #ab40801; Abcam, Cambridge, MA, USA; RRID:AB_731843) and creatine kinase B (mouse monoclonal, 10 μg mL^{-1}, #sc-373686; Santa Cruz Biotechnology, Santa Cruz, CA, USA; RRID:AB_10918186). Western blot analysis using a PR antibody (rabbit polyclonal; dilution 1:250, #A0098; Dako, Glostrup, Denmark; RRID:AB_2315192) was used to determine equal amounts of GST-PR inputs for pull-down assays. GST-PR was further probed as a reference control in pull-down samples. Fluorescent secondary antibodies donkey anti-mouse AF647 (dilution 1:10 000, #A31571; Thermo Fisher Scientific; RRID:AB_162542) were used for SYN2 and creatine kinase B, and donkey anti-rabbit AF546 (dilution 1:10 000; #A10040; Thermo Fisher Scientific; RRID:AB_2534016) for DARPP-32 and PR. Images of immunoreactive bands were taken using a GelDoc Imager (Bio-Rad).

2.9 | In vitro analysis using hiPSCs

2.9.1 | Reagents

P4 (#P6149), E_2 (#E8875) were from Merck (Darmstadt, Germany); SKF 38 393 hydrobromide (#0922) and RU486 (mifepristone; #1479) were from Tocris (St Louis, MO, USA). Pharmacological treatment of cells was performed directly into B27 medium. Drugs were diluted from stock solutions to final concentration in B27 medium; the final

solvent amount was < 0.01%. Vehicle condition consisted of diluting dimethysulphoxide in the same manner as the drugs.

2.10 | hiPSCs

hiPSC lines were generated from primary keratinocytes as described previously.[63] Participants were recruited and methods were carried out in accordance with the 'Patient iPSCs for Neurodevelopmental Disorders (PiNDs) study' (REC No 13/LO/1218) (https://www.hra.nhs.uk/planning-and-improving-research/application-summaries/research-summaries/patient-ipscs-for-neurodevelopmental-disorders-pinds/). Informed consent was obtained from all subjects for participation in the PiNDs study. Ethical approval for the PiNDs study was provided by the NHS Research Ethics Committee at the South London and Maudsley (SLaM) NHS R&D Office. HiPSC lines were derived by reprogramming keratinocytes from healthy males and reprogramming was validated (Table 1) as described previously.[63-66] Briefly, reprograming was validated by genome-wide expression profiling using Illumina Beadchip v4 (Illumina, San Diego, CA, USA) and the bioinformatics tool PLURITEST (Thermo Fisher Scientific). Additionally, the tri-lineage differentiation potential was established by embryoid body formation. Immunocytochemistry was used to validate the expression of different pluripotency markers including Nanog, OCT4, SSEA4 and TRA1-81[65] and alkaline phosphatase activity was assessed by Alkaline phosphatase expression kit (Milipore). The Illumina Human CytoSNP-12v2.1 BeadChip array and analysis using KARYOSTUDIO (Illumina) were used to assess genome integrity (Table 1). hiPSCs were cultured in StemFlex media (#A3349401; Gibco, Gaithersburg, MD, USA) on six-well plates (#140675; Thermo Fisher Scientific) coated with Geltrex basement membrane matrix (#A1413302; Thermo Fisher Scientific). Cells were passaged upon reaching 60%-70% confluency by incubation with a calcium chelator, EDTA (#15040-33; Thermo Fisher Scientific), followed by detachment with a cell lifter to maintain intact iPSC colonies.

2.11 | Neuronal differentiation

Neuronal differentiation of hiPSCs was induced using a modified dual SMAD inhibition protocol.[67] Neural induction was carried out by replacing StemFlex media with a 1:1 mixture of N2 and B27 (Life Technologies, Grand Island, NY, USA) supplemented with 10 μmol L^{-1} SB431542 (Merck), 1 μmol L^{-1} Dorsomorpin (Merck) and 2 μmol L^{-1} XAV939 (Merck) (N2:B27+++ medium). Cells were maintained at 37°C in normoxic conditions in N2:B27+++ medium for 7 days with media replacement every 24 hours. At day 7, cells were dissociated using Accutase (#A11105-01; Life Technologies) and re-plated at a 1:1 ratio into N2:B27+++, supplemented with 10 μmol L^{-1} Rock Inhibitor Y-27632 (Merck) to prevent apoptosis. From day 8 onwards, SMAD and WNT inhibitors were excluded from the medium and cells received daily N2:B27 medium alone. Cells were dissociated and re-plated on days 12, 1, 19 and 21. From day 9, a uniform sheet of Sox2 and Nestin-positive cells was observed and, at day 17, cells were observed to self-organise into neuroepithelial rosettes.[65] On day 21, cells were plated into poly-D-lysine (5 μg mL^{-1}, # P6407; Merck) and laminin (20 μg mL^{-1}, #L2020; Merck) coated eight-well μ-slides (#80826; Ibdi, Gräfelfing, Germany) at a density of 50 000 cell cm^{-2} in B27 medium supplemented with 200 μmol L^{-1} L-ascorbic acid and 10 μmol L^{-1} DAPT (Calbiochem, San Diego, CA, USA) for 7 days (on day 27) to block Notch signalling. Subsequently, neurones were grown in B27 medium with 200 μmol L^{-1} L-ascorbic acid until day 50 when they were used for experimentation. The cells were treated with either E_2 (10 nmol L^{-1}), P4 (1 nmol L^{-1}) or RU486 (10 nmol L^{-1}) for 24 hours prior to harvest. The D1/5 receptor agonist SKF38393 (10 μmol L^{-1}) was applied 30 minutes prior to cell harvest. The six treatment groups were: (i) Veh only; (ii) E_2 only; (iii) E_2 + P4; (iv) E_2 + RU486; (e) E_2 + SKF; and (vi) E_2 + SKF +RU486.

2.12 | Quantitative reverse transcriptase-polymerase chain reaction (RT-PCR)

Total RNA was harvested and lysed with Trizol reagent (Life Technologies) and isolated by centrifugation with 100% chloroform, followed by 100% isopropanol, then 75% ethanol. The RNA was purified by precipitation with 100% ethanol and sodium acetate (Life Technologies). RNA quantity and quality were first analysed using a NanoDrop 1000 Spectrophotometer (Thermo Fisher Scientific). The quality of RNA was further analysed for each sample using the Agilent RNA 6000 Nano Kit (#5067-1511; Agilent Technologies Inc., Santa Clara, CA, USA) in combination with the Agilent 2100 Bioanalyzer system in accordance with the manufacturer's instructions. The RNA integrity number was measured using an Agilent 2100 Bioanalyzer. Residual genomic DNA was removed by addition of TURBO DNA-free (Life Technologies) and incubation at 37°C for 30 minutes. cDNA was synthesised from 1 μg of total RNA using random hexamer primers and SuperScript III (Life Technologies) in accordance with the manufacturer's instructions. A qPCR was performed with HOT FIREPol EvaGreen

TABLE 1 Overview of human-induced pluripotent stem cell quality control[61,64]

hiPSC Line	Age (years)	Sex	Reprogramming method	CytoSNP-12 v2.1	EB Differentiation	Expression of pluripotency markers
CTR_M2_42	30-40	M	Lentivirus	Passed	Passed	Passed
CTR_M3_15	30-40	M	Lentivirus	Passed	Passed	Passed
CTR_M3_22	30-40	M	Lentivirus	Passed	Passed	Passed

qPCR Mix Plus ROX (Solis Biodyne, Tartu, Estonia) in accordance with the manufacturer's instructions in a total volume of 20 μL, containing 1:5 diluted cDNA, qPCR mix and primers at to a final concentration of 0.3 μmol L^{-1}. PCR reaction conditions were 95°C for 15 minutes for the initial denaturation followed by 95°C for 30 seconds, 60°C for 30 seconds and 72°C for 30 seconds during 33 cycles. The melting curve analyses was preformed from 60°C to 95°C with readings every 1°C. The 2^ ΔΔ CT comparative method for relative quantification was used to quantify gene expression. To determine the appropriate housekeeping genes for normalisation of the qPCR data, *ACTB*, *B2M*, *GAPDH*, *HMBS*, *HPRT1*, *RPL13A*, *RPL27*, *SDHA*, *UBC* and *YWHAZ* were screened for efficiency and specificity in the hiPSC lines at multiple times over neuronal differentiation towards a GnRH-neuronal identity. All genes were assayed by determining the relative quantification of the gene expression between hiPSC samples. Based on this analysis, *GAPDH* was chosen as the reference gene because it displayed the lowest variability in expression levels between multiple (×4) hiPSC lines and across all time points assessed.

2.13 | Immunocytochemistry

Treated neurones were fixed with 4% formaldehyde plus 4% sucrose in phosphate-buffered saline (PBS). Fixed neurones were permeabilised in 0.1% Triton-X-100 in PBS for 15 minutes and blocked in 4% normal goat serum in PBS for 1 hour at room temperature. Cells were incubated overnight in appropriate primary antibodies at 4°C. The rabbit polyclonal primary antibodies for GnRH (dilution 1:200; #HPA027532; Atlas, Stockholm, Sweden; RRID:AB_10612111), tyrosine hydroxylase (TH; dilution 1:200; #ab152; Millipore; RRID:AB_390204) and vasopressin (dilution 1:100; #ab6869; Abcam; RRID:AB_2062094) were used to confirm the hypothalamic-like phenotype of the hiPSC neurones. A chicken polyclonal Tuj1 antibody (dilution 1:500; #ab41489; Abcam; RRID:AB_727049) was used as a neuronal marker and a rabbit polyclonal MAP2 antibody (dilution 1:1000; #ab32454; Abcam; RRID:AB_776174) was used to outline neuronal morphology. Progesterone receptor and SYN1/2 expression in the hiPSC neurones were confirmed using a mouse monoclonal (dilution 1:500; #MA5-12658; Invitrogen; RRID:AB_11000632) and a chicken polyclonal (dilution 1:1000; #106006; Synaptic Systems, Goettingen, Germany; RRID:AB_2622240) primary antibodies, respectively. Immunoreactivity was achieved by incubating the cells with a 1:500 concentration of Alexa Fluor 594 anti-mouse, Alexa Fluor 594 anti-goat and Alexa Fluor 488 anti-rabbit IgGs in blocking buffer. For nuclei staining, a 1:2000 concentration of 4',6-diamidino-2-phenylindole (DAPI) (Thermo Fisher Scientific) was used.

2.14 | Microscopy and image analysis

Confocal images were taken as z-stacks with a SP5 laser scanning confocal microscope (Leica Microsystems, Wetzlar, Germany) equipped with 405/488/594nm lasers and using a 63× NA1.4 objective. Identical laser gain and offset settings were used within each biological replicate to enable direct comparison between conditions. Two-dimensional maximum projection reconstructions of images were generated and intensity analyses were performed using IMAGEJ (rsb.info.nih.gov/ij). In all images, MAP2 was used to identify neurones and outline neuronal morphology. The mean grey value of PR intensity was measured within the cell body and along the first 10 μm of each neurone analysed. SYN1/2 intensity (mean grey value) was measured along 50 μm of dendrite from each neurone analysed. In all experiments, three clones per hiPSC line were used; each clonal line was used in at least two independent differentiation for each condition imaged and analysed: 18-30 neurones per condition were analysed.

2.15 | Statistical analysis

All statistical analyses were performed in PRISM (GraphPad Software Inc., San Diego, CA, USA) (RRID:SCR_000306). All data sets were tested for normality using the D'Agostino & Pearson normality test prior to inferential statistical analyses[68]. Datasets were found to be normally distributed, thus were measured by one-way ANOVA with Tukey's post-hoc test to correct for multiple comparisons. $P < 0.05$ was considered statistically significant. Error bars represent either the SD or SEM, as indicated in the figure legends.

3 | RESULTS

3.1 | Mass spectrometry reveals an interaction between PR-A and hypothalamic proteins from SKF-treated mice

To test whether PR-A or PR-B, in the absence of P4, interact with proteins from the female mouse hypothalamus in a DA-dependent manner, a D1R agonist, SKF, was infused into the third ventricle. Mouse GST-PR-A and GST-PR-B were separately used to pull-down hypothalamic proteins from SKF or Veh-treated female mice. Prior to statistical analyses, 525 and 281 proteins were detected to interact with unliganded PR-A and unliganded PR-B, respectively. Given that the focus of the present study was the identification of the SKF-dependent PR interactome, applying a cut-off of $P < 0.05$ and an at least two-fold change yielded 316 hypothalamic proteins from SKF-treated mice that interacted with GST-PR-A compared to Veh mice (Table 2). Interestingly, none of the 281 proteins that interacted with unliganded PR-B did so in an SKF-dependent manner, suggesting limited involvement of PR-B in DA activation of PR. Although many identified proteins are known to exert multiple functions, proteins were functionally grouped based on their primary functions in UniProt database (http://uniprot.org). As shown in Table 2, the largest number of proteins are important for synaptic structure and function (62 out of 316; 20%). Other groups, including members of cytoskeleton, calcium regulation, electron transfer/ion channel and cell signalling, all known to be classically involved in synaptic transmission and plasticity,

were also identified. The second largest functional group of proteins that interacted with PR-A in an SKF-dependent manner are involved in cellular and energy metabolism (57 out of 316; 18%). In addition, regulators of transcription, translation, ubiquitination, protein folding/molecular chaperones, and cell proliferation were identified in the SKF-dependent PR-A interactome (Table 2).

3.2 | Synaptic proteins from SKF-treated female mouse hypothalamus interact with PR-A

Extending our earlier findings that showed that synaptic proteins interacted with ligand-activated PR,[16] in the present study, we identified a large number of synaptic proteins that interacted with PR-A in a ligand-independent but DA-dependent manner (Table 2). For example, many synaptic terminal proteins such as synaptophysin, β-synuclein, γ-synuclein and synaptotagmin-1 from SKF-treated hypothalamus interacted with PR-A. In addition, proteins implicated in synaptic vesicle exocytosis, such as SYN2, SYN3, synaptic vesicle membrane protein VAT-1 homologue-like (VAT1L), synaptosomal-associated protein 25 (SNAP25), amphiphysin, vesicle-associated membrane protein (VAMP)1 and VAMP2 also showed DA-dependent interactions with PR-A. Moreover, proteins necessary for neurotransmitter synthesis (eg aspartate aminotransferase (AATC), proSAAS), neurotransmitter turnover (eg glutamate decarboxylase 2 [DCE2], glutamine synthetase [GLNA], 4-aminobutyrate aminotransferase [GABT], succinate-semialdehyde dehydrogenase [SSDH] and glutamate dehydrogenase 1 [DHE3]) and neurotransmitter transport (excitatory amino acid transporter [EAA]1 and EAA2) from SKF-treated hypothalamus preferentially interacted with PR-A compared to the Veh-treated mice. Consistent with the role of Ca^{2+} regulation on synaptic neurotransmitter release, a number of Ca^{2+}-dependent proteins also showed a DA-dependent interaction with PR-A (Table 2). In addition, transporter proteins interacted with PR-A suggesting a role for the receptor in synaptic transmission (Table 2). Other functional groups, including kinases and phosphatases, and their diverse substrates (eg, those belonging to cytoskeletal proteins, ubiquitination enzymes, ion channel proteins and molecular chaperones) interacted with PR-A in a DA-dependent manner.

3.3 | Regulators of energy metabolism from mouse hypothalamus interact with PR-A in an SKF-dependent manner

The current interactome data suggest that PR-A-dependent regulation of energy metabolism is extensive and involves enzymes necessary at multiple steps of energy metabolism, including glycolysis, tricarboxylic acid (TCA) cycle, oxidative phosphorylation, gluconeogenesis and glycogenolysis (Table 2). The mediators of glycolysis (including glyceraldehyde-3-phosphate dehydrogenase [G3P], glucose 6-phosphate isomerase, glucose 6-phosphate isomerase [G6PI], phosphoglycerate kinase 1, pyruvate kinase PKM, 6-phosphofructokinase [type C and muscle type]) from SKF-treated, but not Veh-treated, mouse hypothalamus interacted with PR-A. The enzymes required for the TCA cycle, such as citrate synthase, malate dehydrogenase, aconitate hydratase, fumarate hydratase and isocitrate dehydrogenase a (IDH3A), interacted with PR-A in a DA-dependent manner. Proteins integral in oxidative phosphorylation, including dihydrolipoyl dehydrogenase, cytochrome C, ATP synthase A, ATP synthase B, succinyl-CoA ligase A and malate dehydrogenase, also showed DA-dependent interactions with mouse PR-A. In addition, proteins that protect cells against oxidative stress, such as peroxiredoxin [PRDX]1, PRDX2, PRDX5 and PRDX6 from SKF-treated hypothalamus, preferentially interacted with PR-A. Additionally, proteins required for gluconeogenesis (eg L-lactate dehydrogenase [LDH]A and LDHB), glycogen utilisation (eg, glycogen phosphorylase brain form [PYGB] and phosphoglucomutase-1 [PGM1] and pyruvate metabolism [eg, pyruvate dehydrogenase E1B], all showed an SKF-dependent interaction with PR-A. Other proteins, such as apolipoprotein E, acetyl-CoA acetyltransferase, fatty acid synthase and enoyl-CoA hydratase, which are integral for lipid metabolism, also preferentially interacted with PR-A in a SKF-dependent manner.

3.4 | PR-A-interacting mouse hypothalamic protein networks

The network pathway for synaptic proteins (Figure 2) and metabolic regulators (Figure 3) generated using Ingenuity pathway analysis revealed that the majority of these proteins form complexes with, or directly act (solid lines) on other identified proteins, whereas a smaller subset of these proteins act indirectly (dotted lines) with other proteins in the network. In addition, many proteins in these functional groups possess auto-regulatory mechanisms (indicated by an incomplete circle in Figures 2 and 3) by direct auto-regulation (arrow) or by forming complexes with themselves (no arrow). The networks provided further evidence of the functional interactions of the synaptic proteins and metabolic regulators identified in the present study.

3.5 | PR-A interaction with select hypothalamic proteins were verified by western blotting

For the qualitative validation of findings from MS, proteins from SKF- or Veh-treated hypothalami pulled down using PR-A were analysed by western blotting. Consistent with the MS results, a more intense creatine kinase B immunoreactive band (approximately 45 kDa) was detected in pull-downs with SKF-treated samples compared with Veh-treated tissue (Figure 4). DARPP-32 (approximately 35kDa), a protein critical for DA-mediated activation of PR in brain and for mediation of female sexual receptivity,[55] from SKF-treated hypothalamus also interacted strongly with PR-A compared to Veh-treated hypothalamus. Moreover, SYN2b, and to a lesser extent SYN2a, interacted with unliganded PR-A in an SKF-dependent manner, together confirming DA-dependent interactions of these proteins with

TABLE 2 Proteins from female mouse hypothalamus associate with unliganded PR-A in an SKF-dependent manner as identified by mass spectrometry

UniProt ID	*P* values	Fold change SKF/Veh	Protein name
Synaptic proteins			
SYUG	0.00006	9.40	Gamma-synuclein
EAA1	0.00001	6.71	Excitatory amino acid transporter 1
EAA2	0.00002	5.89	Excitatory amino acid transporter 2
NCAM1	0.00156	5.78	Neural cell adhesion molecule 1
RAC1	0.01584	5.61	Ras-related C3 botulinum toxin substrate 1
GABT	0.00001	5.58	4-aminobutyrate aminotransferase, mitochondrial
VAT1L	0.00105	5.35	Synaptic vesicle membrane protein VAT-1 homologue-like
DNM1L	0.00274	4.64	Dynamin-1-like protein
SCG2	0.00589	4.57	Secretogranin-2
PCSK1	0.00236	4.50	ProSAAS
DLG2	0.00993	4.35	Disks large homologue 2
SSDH	0.00009	4.34	Succinate-semialdehyde dehydrogenase, mitochondrial
PAK1	0.01048	4.27	Serine/threonine-protein kinase PAK 1
SNP25	0.00911	4.20	Synaptosomal-associated protein 25
SYN3	0.01122	3.94	Synapsin III
ANXA6	0.00058	3.93	Annexin A6
NFM	0.00001	3.87	Neurofilament medium polypeptide
SH3G2	0.00018	3.79	Endophilin-A1
AMPH	0.00162	3.77	Amphiphysin
SEPT5	0.01209	3.71	Septin-5
AATC	0.00000	3.60	Aspartate aminotransferase, cytoplasmic
STMN1	0.00029	3.55	Stathmin
STX1B	0.00205	3.53	Syntaxin-1B
NEUM	0.00238	3.37	Neuromodulin
SYUB	0.01278	3.33	Beta-synuclein
VAMP1	0.00304	3.32	Vesicle-associated membrane protein 1
RAB3A	0.00022	3.27	Ras-related protein Rab-3A
SYNJ1	0.00150	3.25	Synaptojanin-1
STXB1	0.00024	3.24	Syntaxin-binding protein 1
ACTZ	0.00731	3.23	Alpha-centractin
NCDN	0.00058	3.16	Neurochondrin
VAMP2	0.02680	3.14	Vesicle-associated membrane protein 2
RAB1A	0.00356	3.12	Ras-related protein Rab-1A
PACN1	0.00030	3.05	Protein kinase C and casein kinase substrate in neurones protein 1
SEPT7	0.00134	2.98	Septin-7
SEPT6	0.01040	2.98	Septin-6
DHE3	0.00181	2.89	Glutamate dehydrogenase 1, mitochondrial
1433B	0.00320	2.86	14-3-3 protein beta/alpha
SYPH	0.01134	2.85	Synaptophysin
DPYL5	0.00006	2.82	Dihydropyrimidinase-related protein 5
SYN2	0.00005	2.82	Synapsin II
SYT1	0.00457	2.74	Synaptotagmin-1

(Continues)

TABLE 2 (Continued)

UniProt ID	*P* values	Fold change SKF/Veh	Protein name
1433T	0.00069	2.74	14-3-3 protein theta
DPYL1	0.00041	2.71	Dihydropyrimidinase-related protein 1
DCE2	0.00681	2.65	Glutamate decarboxylase 2
THY1	0.02158	2.65	Thy-1 membrane glycoprotein
1433E	0.00003	2.61	14-3-3 protein epsilon
1433Z	0.00075	2.61	14-3-3 protein zeta/delta
1433F	0.00515	2.60	14-3-3 protein eta
DYN3	0.04836	2.59	Dynamin-3
GLNA	0.00032	2.57	Glutamine synthetase
DYN1	0.00035	2.56	Dynamin-1
ASGL1	0.03685	2.51	Isoaspartyl peptidase/L-asparaginase
FMR1	0.00819	2.51	Fragile X mental retardation protein 1 homologue
NSF	0.01810	2.49	Vesicle-fusing ATPase
SNAB	0.04630	2.48	Beta-soluble NSF attachment protein
SEPT11	0.01801	2.41	Septin-11
TENR	0.00098	2.40	Tenascin-R
CPLX2	0.02331	2.18	Complexin-2
1433G	0.00202	2.17	14-3-3 protein gamma
DYL2	0.02540	2.13	Dynein light chain 2, cytoplasmic
PPR1B/ DARPP32	0.02664	2.13	Protein phosphatase 1 regulatory subunit 1B
Cytoskeletons			
CAPZB	0.00240	8.20	F-actin-capping protein subunit beta
SRR	0.00379	6.35	Serine racemase
TYB4	0.00001	5.25	Thymosin beta-4
AINX	0.00794	4.31	Alpha-internexin
ARP3	0.00154	4.24	Actin-related protein 3
LASP1	0.00187	4.21	LIM and SH3 domain protein 1
PROF1	0.00317	4.09	Profilin-1
ADDA	0.00114	4.08	Alpha-adducin
SPTB2	0.00312	4.05	Spectrin beta chain, non-erythrocytic 1
DREB	0.04358	3.96	Drebrin
PROF2	0.02067	3.96	Profilin-2
NFL	0.00029	3.59	Neurofilament light polypeptide
ATOX1	0.00041	3.48	Copper transport protein ATOX1
SPTN1	0.00065	3.42	Spectrin alpha chain, non-erythrocytic 1
CAZA2	0.01274	3.34	F-actin-capping protein subunit alpha-2
COR1C	0.00030	3.30	Coronin-1C
MARE3	0.02173	3.22	Microtubule-associated protein RP/EB family member 3
COF1	0.00014	3.21	Cofilin-1
DPYL3	0.00002	3.12	Dihydropyrimidinase-related protein 3
ACTS	0.01717	2.95	Actin, alpha skeletal muscle
ACTG	0.00004	2.90	Actin, cytoplasmic 2
TAU	0.00002	2.81	Microtubule-associated protein tau
CAP1	0.00010	2.67	Adenylyl cyclase-associated protein 1

(Continues)

TABLE 2 (Continued)

UniProt ID	*P* values	Fold change SKF/Veh	Protein name
TPPP	0.00001	2.60	Tubulin polymerisation-promoting protein
COF2	0.00123	2.55	Cofilin-2
E41L1	0.00222	2.52	Band 4.1-like protein 1
TBB3	0.00009	2.51	Tubulin beta-3 chain
FSCN1	0.00301	2.38	Fascin
TPPP3	0.01691	2.32	Tubulin polymerisation-promoting protein family member 3
TBB4B	0.00104	2.32	Tubulin beta-4B chain
MAP1B	0.00004	2.28	Microtubule-associated protein 1B
TBB5	0.00098	2.23	Tubulin beta-5 chain
MTPN	0.04620	2.17	Myotrophin
TBB2B	0.00003	2.06	Tubulin beta-2B chain
TBA4A	0.00492	2.06	Tubulin alpha-4A chain
Calcium regulation			
CALR	0.00020	4.51	Calreticulin
PCP4	0.00042	4.24	Purkinje cell protein 4
S100B	0.00007	4.14	Protein S100-B
CALB2	0.00021	4.10	Calretinin
KPCB	0.03848	4.04	Protein kinase C beta type
PGCB	0.00021	3.65	Brevican core protein
EPDR1	0.01366	3.65	Mammalian ependymin-related protein 1
SCRN1	0.00021	3.65	Secernin-1
ANK2	0.00047	3.57	Ankyrin-2
KCC2B	0.00215	2.78	Calcium/calmodulin-dependent protein kinase type II subunit beta
CANB1	0.01520	2.26	Calcineurin subunit B-type 1
PP2BA	0.00123	2.25	Serine/threonine-protein phosphatase 2B catalytic subunit alpha isoform
KCC2A	0.01272	2.24	Calcium/calmodulin-dependent protein kinase type II subunit alpha
CALM	0.00072	2.23	Calmodulin
AT2B2	0.00438	6.86	Plasma membrane calcium-transporting ATPase 2
Electron transfer/ion channel			
ETFA	0.00037	8.23	Electron transfer flavoprotein subunit alpha, mitochondrial
VATE1	0.03893	7.37	V-type proton ATPase subunit E 1
AT1A1	0.00258	7.24	Sodium/potassium-transporting ATPase subunit alpha-1
AT1A2	0.00039	6.59	Sodium/potassium-transporting ATPase subunit alpha-2
AT2A2	0.00813	6.35	Sarcoplasmic/endoplasmic reticulum calcium ATPase 2
ETFB	0.00561	6.27	Electron transfer flavoprotein subunit beta
VATG2	0.00186	4.89	V-type proton ATPase subunit G 2
AT1B1	0.00252	4.35	Sodium/potassium-transporting ATPase subunit beta-1
AT1A3	0.00011	4.32	Sodium/potassium-transporting ATPase subunit alpha-3
VPP1	0.03177	4.10	V-type proton ATPase 116 kDa subunit a isoform 1
VATH	0.00005	4.01	V-type proton ATPase subunit H
Cell signalling			
PEA15	0.00889	9.81	Astrocytic phosphoprotein PEA-15
CNTN1	0.02587	4.29	Contactin-1

(Continues)

TABLE 2 (Continued)

UniProt ID	*P* values	Fold change SKF/Veh	Protein name
MP2K1	0.00984	3.50	Dual specificity mitogen-activated protein kinase kinase 1
NDKA	0.00011	3.49	Nucleoside diphosphate kinase A
KAP3	0.01949	3.32	cAMP-dependent protein kinase type II-beta regulatory subunit
GLOD4	0.00364	3.27	Glyoxalase domain-containing protein 4
MYPR	0.00025	3.13	Myelin proteolipid protein
GNAO	0.01483	3.02	Guanine nucleotide-binding protein G(o) subunit alpha
CNRP1	0.00814	2.90	CB1 cannabinoid receptor-interacting protein 1
GBB1	0.00024	2.64	Guanine nucleotide-binding protein G(I)/G(S)/G(T) subunit beta-1
DUS3	0.01265	2.61	Dual specificity protein phosphatase 3
2AAA	0.00042	2.24	Serine/threonine-protein phosphatase 2A 65-kDa regulatory subunit A alpha isoform
Transporters			
7B2	0.00022	7.45	Neuroendocrine protein 7B2
TRFE	0.01112	5.32	Serotransferrin
THTR	0.02611	4.12	Thiosulphate sulphurtransferase
RAB14	0.00553	3.94	Ras-related protein Rab-14
LIS1	0.00016	3.89	Platelet-activating factor acetylhydrolase IB subunit alpha
ALBU	0.00018	3.79	Serum albumin
GDIB	0.00005	3.62	Rab GDP dissociation inhibitor beta
ACBP	0.00308	3.49	Acyl-CoA-binding protein
GDIA	0.00001	3.32	Rab GDP dissociation inhibitor alpha
VATA	0.00000	3.27	V-type proton ATPase catalytic subunit A
AP180	0.00020	3.26	Clathrin coat assembly protein AP180
RAN	0.00012	3.20	GTP-binding nuclear protein Ran
VPS35	0.00400	3.20	Vacuolar protein sorting-associated protein 35
GDIR1	0.00461	3.20	Rho GDP dissociation inhibitor 1
VATB2	0.00164	2.91	V-type proton ATPase subunit B, brain isoform
HBB1	0.00402	2.72	Hemoglobin subunit beta-1
HBA	0.00010	2.61	Hemoglobin subunit alpha
CLH1	0.00063	2.49	Clathrin heavy chain 1
AAK1	0.01983	2.15	AP2-associated protein kinase 1
DYL2	0.02540	2.13	Dynein light chain 2, cytoplasmic
Cellular and energy metabolism			
TRXR1	0.00478	14.02	Thioredoxin reductase 1, cytoplasmic
ECHM	0.02149	8.45	Enoyl-CoA hydratase, mitochondrial
MAOX	0.00189	7.74	NADP-dependent malic enzyme
GRHPR	0.03647	6.60	Glyoxylate reductase/hydroxypyruvate reductase
SERC	0.00060	5.67	Phosphoserine aminotransferase
FABP5	0.00342	5.60	Fatty acid-binding protein, epidermal
FA49B	0.01836	5.60	Protein FAM49B
FAS	0.00002	5.51	Fatty acid synthase
FABPH	0.00607	5.51	Fatty acid-binding protein, heart
LDHA	0.00001	5.39	L-lactate dehydrogenase A chain
ACYP1	0.00257	5.29	Acylphosphatase-1

(Continues)

TABLE 2 (Continued)

UniProt ID	*P* values	Fold change SKF/Veh	Protein name
KAD1	0.00036	4.84	Adenylate kinase isoenzyme 1
PLPP	0.04142	4.68	Pyridoxal phosphate phosphatase
IDH3A	0.00101	4.35	Isocitrate dehydrogenase [NAD] subunit alpha, mitochondrial
BACH	0.00000	4.33	Cytosolic acyl coenzyme A thioester hydrolase
PRDX6	0.00528	3.88	Peroxiredoxin-6
PGM1	0.00012	3.87	Phosphoglucomutase-1
PDXK	0.00009	3.82	Pyridoxal kinase
PGK1	0.00027	3.64	Phosphoglycerate kinase 1
6PGD	0.02056	3.49	6-phosphogluconate dehydrogenase, decarboxylating
G6PI	0.00007	3.49	Glucose 6-phosphate isomerase
DLDH	0.00196	3.48	Dihydrolipoyl dehydrogenase, mitochondrial
ENOA	0.00000	3.45	Alpha-enolase
TPIS	0.00001	3.34	Triosephosphate isomerase
AATM	0.00279	3.31	Aspartate aminotransferase, mitochondrial
PP1G	0.00009	3.31	Serine/threonine-protein phosphatase PP1-gamma catalytic subunit
ALDOC	0.00000	3.28	Fructose-bisphosphate aldolase C
PEBP1	0.00127	3.22	Phosphatidylethanolamine-binding protein 1
DHPR	0.01434	3.22	Dihydropteridine reductase
ALDOA	0.00033	3.12	Fructose-bisphosphate aldolase A
KPYM	0.00000	3.11	Pyruvate kinase PKM
PRDX2	0.00478	3.03	Peroxiredoxin-2
KCRB	0.00004	3.00	Creatine kinase B-type
FUMH	0.00182	2.99	Fumarate hydratase, mitochondrial
G3P	0.00065	2.99	Glyceraldehyde-3-phosphate dehydrogenase
IPYR	0.01978	2.97	Inorganic pyrophosphatase
MDHC	0.00074	2.93	Malate dehydrogenase, cytoplasmic
ATPA	0.00151	2.92	ATP synthase subunit alpha, mitochondrial
ODP2	0.00713	2.89	Dihydrolipoyllysine-residue acetyltransferase component of pyruvate dehydrogenase complex, mitochondrial
CISY	0.00139	2.88	Citrate synthase, mitochondrial
CYC	0.00306	2.88	Cytochrome *c*, somatic
HXK1	0.00059	2.87	Hexokinase-1
PYGB	0.01142	2.80	Glycogen phosphorylase, brain form
K6PF	0.00324	2.77	6-phosphofructokinase, muscle type
MDHM	0.00011	2.76	Malate dehydrogenase, mitochondrial
ODPB	0.01496	2.73	Pyruvate dehydrogenase E1 component subunit beta, mitochondrial
APOE	0.03085	2.68	Apolipoprotein E
TALDO	0.00223	2.66	Transaldolase
LDHB	0.00001	2.66	L-lactate dehydrogenase B chain
THIL	0.00005	2.62	Acetyl-CoA acetyltransferase, mitochondrial
PRDX5	0.00062	2.60	Peroxiredoxin-5, mitochondrial

(Continues)

TABLE 2 (Continued)

UniProt ID	*P* values	Fold change SKF/Veh	Protein name
ATPB	0.00023	2.54	ATP synthase subunit beta, mitochondrial
PRDX1	0.00048	2.51	Peroxiredoxin-1
SUCA	0.00700	2.44	Succinyl-CoA ligase [ADP/GDP-forming] subunit alpha, mitochondrial
ACON	0.00059	2.42	Aconitate hydratase, mitochondrial
K6PP	0.00023	2.38	6-phosphofructokinase type C
ACLY	0.03720	2.35	ATP-citrate synthase
Other enzymes			
ESTD	0.00970	8.57	*S*-formylglutathione hydrolase
SPRE	0.03523	6.71	Sepiapterin reductase
ADHX	0.01662	6.39	Alcohol dehydrogenase class-3
CAH2	0.00003	4.13	Carbonic anhydrase 2
DDAH1	0.00042	3.99	*N*(G),*N*(G)-dimethylarginine dimethylaminohydrolase 1
CRYM	0.00005	3.97	Ketimine reductase mu-crystallin
HDHD2	0.00043	3.96	Haloacid dehalogenase-like hydrolase domain-containing protein 2
PGAM1	0.00005	3.86	Phosphoglycerate mutase 1
AL7A1	0.00408	3.81	Alpha-aminoadipic semialdehyde dehydrogenase
PSA	0.00002	3.74	Puromycin-sensitive aminopeptidase
AK1A1	0.01651	3.74	Alcohol dehydrogenase [NADP(+)]
TKT	0.00097	3.68	Transketolase
ASSY	0.02263	3.37	Argininosuccinate synthase
DPYL4	0.01193	3.30	Dihydropyrimidinase-related protein 4
ENOG	0.00005	3.24	Gamma-enolase
SODC	0.00050	3.15	Superoxide dismutase [Cu-Zn]
LGUL	0.00840	3.15	Lactoylglutathione lyase
PPCEL	0.00363	2.91	Prolyl endopeptidase-like
DPYL2	0.00020	2.89	Dihydropyrimidinase-related protein 2
GUAD	0.00334	2.60	Guanine deaminase
CN37	0.00801	2.27	2',3'-cyclic-nucleotide 3'-phosphodiesterase
Transcription			
KCY	0.00520	6.56	UMP-CMP kinase
NT5C	0.00342	6.31	5'(3')-deoxyribonucleotidase, cytosolic type
AN32A	0.00020	4.75	Acidic leucine-rich nuclear phosphoprotein 32 family member A
AP1B1	0.00034	4.18	AP-1 complex subunit beta-1
TAGL3	0.00019	4.00	Transgelin-3
EFTU	0.02217	3.56	Elongation factor Tu, mitochondrial
ARF3	0.00418	3.47	ADP-ribosylation factor 3
NDRG2	0.00055	3.45	Protein NDRG2
NSF1C	0.00509	3.34	NSFL1 cofactor p47
AP2A2	0.00067	3.04	AP-2 complex subunit alpha-2
HMGB1	0.01268	2.88	High mobility group protein B1
BASP1	0.00021	2.52	Brain acid soluble protein 1
CSRP1	0.00668	2.45	Cysteine and glycine-rich protein 1
AP2A1	0.00001	2.22	AP-2 complex subunit alpha-1

(Continues)

TABLE 2 (Continued)

UniProt ID	*P* values	Fold change SKF/Veh	Protein name
HNRPK	0.00124	2.09	Heterogeneous nuclear ribonucleoprotein K
AP2B1	0.01957	2.09	AP-2 complex subunit beta
DDX17	0.00002	2.08	Probable ATP-dependent RNA helicase DDX17
Translation			
IF5A1	0.00534	6.70	Eukaryotic translation initiation factor 5A-1
UK114	0.00157	4.40	Ribonuclease UK114
SYWC	0.00209	3.97	Tryptophan--tRNA ligase, cytoplasmic
IMPCT	0.00090	3.92	Protein IMPACT
TSR2	0.01589	3.69	Pre-rRNA-processing protein TSR2 homologue
RL23	0.00001	3.26	60S ribosomal protein L23
IF4H	0.00011	3.04	Eukaryotic translation initiation factor 4H
RS23	0.01866	2.66	40S ribosomal protein S23
RL9	0.03345	2.53	60S ribosomal protein L9
RS8	0.04217	2.29	40S ribosomal protein S8
RS11	0.02283	2.25	40S ribosomal protein S11
FBLL1	0.00730	2.23	rRNA/tRNA 2'-*O*-methyltransferase fibrillarin-like protein 1
PABP1	0.04778	2.20	Polyadenylate-binding protein 1
FBRL	0.00028	2.04	rRNA 2'-*O*-methyltransferase fibrillarin
IF4A2	0.03558	2.01	Eukaryotic initiation factor 4A-II
Ubiquitination			
PSA5	0.00714	4.27	Proteasome subunit alpha type-5
UBP5	0.00247	4.20	Ubiquitin carboxyl-terminal hydrolase 5
PIMT	0.03321	9.71	Protein-L-isoaspartate(D-aspartate) *O*-methyltransferase
NEDD8	0.00568	7.10	NEDD8
THOP1	0.02828	4.67	Thimet oligopeptidase
UBA1	0.00002	3.98	Ubiquitin-like modifier-activating enzyme 1
UB2L3	0.00005	3.66	Ubiquitin-conjugating enzyme E2 L3
UCHL1	0.00013	3.46	Ubiquitin carboxyl-terminal hydrolase isozyme L1
PCBP2	0.00116	3.39	Poly(rC)-binding protein 2
UB2D2	0.00642	3.39	Ubiquitin-conjugating enzyme E2 D2
PCBP1	0.02341	3.07	Poly(rC)-binding protein 1
OTUB1	0.02514	3.04	Ubiquitin thioesterase OTUB1
CAND1	0.00895	3.00	Cullin-associated NEDD8-dissociated protein 1
UBE2N	0.00618	3.00	Ubiquitin-conjugating enzyme E2 N
CYTB	0.00919	2.95	Cystatin-B
PSA1	0.01733	2.93	Proteasome subunit alpha type-1
PSA7	0.00042	2.88	Proteasome subunit alpha type-7
HINT1	0.00011	2.86	Histidine triad nucleotide-binding protein 1
WDR1	0.00569	2.73	WD repeat-containing protein 1
BIN1	0.01992	2.70	Myc box-dependent-interacting protein 1
UBC	0.00113	2.25	Polyubiquitin-C
MIF	0.00056	2.39	Macrophage migration inhibitory factor

(Continues)

TABLE 2 (Continued)

UniProt ID	*P* values	Fold change SKF/Veh	Protein name
Cell proliferation			
TCTP	0.00338	12.87	Translationally-controlled tumour protein
GUAA	0.00426	5.96	GMP synthase [glutamine-hydrolysing]
TPRGL	0.00790	5.02	Tumour protein p63-regulated gene 1-like protein
HPRT	0.00115	4.50	Hypoxanthine-guanine phosphoribosyltransferase
SAHH2	0.00194	3.84	Putative adenosylhomocysteinase 2
TERA	0.00003	3.67	Transitional endoplasmic reticulum ATPase
E41L3	0.00370	2.96	Band 4.1-like protein 3
DTD1	0.00042	2.49	D-tyrosyl-tRNA(Tyr) deacylase 1
Protein folding/molecular chaperones			
TCPA	0.00211	6.77	T-complex protein 1 subunit alpha
COTL1	0.00194	5.63	Coactosin-like protein
PTPA	0.01297	4.08	Serine/threonine-protein phosphatase 2A activator
FKB1A	0.00136	3.86	Peptidyl-prolyl cis-trans isomerase FKBP1A
CYTC	0.01739	3.63	Cystatin-C
TCPZ	0.01058	3.57	T-complex protein 1 subunit zeta
PDIA3	0.00294	3.29	Protein disulphide-isomerase A3
TCPB	0.00363	3.24	T-complex protein 1 subunit beta
CH10	0.00034	3.21	10-kDa heat shock protein, mitochondrial
PARK7	0.00603	3.16	Protein DJ-1
TEBP	0.00124	2.94	Prostaglandin E synthase 3
TCPD	0.00091	2.92	T-complex protein 1 subunit delta
TCPQ	0.00508	2.79	T-complex protein 1 subunit theta
PDIA1	0.00773	2.78	Protein disulphide-isomerase
TCPE	0.01844	2.76	T-complex protein 1 subunit epsilon
PPIA	0.00483	2.62	Peptidyl-prolyl cis-trans isomerase A
F10A1	0.01592	2.57	Hsc70-interacting protein
HS90A	0.00037	2.52	Heat shock protein HSP 90-alpha
HS90B	0.00195	2.45	Heat shock protein HSP 90-beta
STIP1	0.00782	2.44	Stress-induced-phosphoprotein 1
CH60	0.00250	2.21	60-kDa heat shock protein, mitochondrial
Total: 316			

Proteins are assigned functional groups based on their known primary function. In total, 316 proteins that associate with unliganded GST-PR-A with an SKF/Veh ratio ≥ 2 and $P < 0.05$ by a *t* test are included.

PR-A. Similar intensities of PR-A bands were observed in SKF and Veh lanes, confirming equal amounts of protein loaded in each pull-down assay (Figure 4).

3.6 | Generation of hypothalamic-like neurones from hiPSCs

Because the largest group of hypothalamic proteins that interacted with PR were synaptic proteins, including SYN1/2, we investigated whether PR and SYN1/2 were co-expressed and regulated in neuronal processes, including dendrites. The present PR interactome data, taken together with previous findings,[16] indicate that DA-dependent modulation of synaptic protein expression requires E_2-induced PR. Therefore, we generated a population of olfactory placode progenitor cells from hiPSCs, which subsequently could be differentiated into a population of hypothalamic-like GnRH-positive neurones that express E_2-induced PR,[65,69-71] aiming to test the DA-dependent functional interaction between the PR and synaptic proteins.

HiPSC lines were derived by reprogramming keratinocytes from healthy males (Table 1) as described previously.[63-66] HiPSC lines were differentiated into neuroepithelial cells using a modified dual SMAD

inhibition differentiation protocol (Figure 5A) as described previously.[63] QPCR analyses demonstrated that the neuroepithelial marker *SOX2* was highly expressed at day 7 and was gradually down-regulated during the 50 days of neuronal fate acquisition (Figure 5B). *PAX6*, a marker of forebrain development, was highly expressed from day 7 to 20, when cells were terminally differentiated. After this time point, *PAX6* levels were greatly reduced in the cells (Figure 5C). A hypothalamic-like identity of these cells was confirmed by the high expression of the transcription factor NK2 homeobox 1 (*NKX2.1*) in day 12 and 18 neural progenitor cells (NPCs) (Figure 5D).[72,73] We also found that *LHX6*, a factor known to be involved in hypothalamic specification [74,75] was highly expressed in NPCs (Figure 5D).

We next confirmed the generation of GnRH-positive hiPSC neurones by qPCR; *GnRH* was expressed highly in day 26 and 50 neurones (Figure 5E). Interestingly, the expression of oestrogen receptor genes *ESR1* and *ESR2* increased between the early time point and older, day 50, neurones (Figure 5E). Immunocytochemical analysis at day 26 further confirmed that the majority of cells generated were positive for β-III tubulin (Tuj1), a marker of neuronal fate, and highly expressed GnRH, tyrosine hydroxylase (TH) and vasopressin (Figure 5F). Taken together, these data suggest the successful generation of GnRH-positive hypothalamic-like neurones (hiPSC neurones).

3.7 | Oestradiol induces PR expression in GnRH-expressing hiPSC neurones

GnRH-positive hiPSC neurones generated from male hiPSCs responded to E_2 treatment with a significant increase in PR expression (Figure 6A,B). Because a large number of synaptic proteins from SKF-treated hypothalamus interacted with PR-A, we next investigated whether PR is localised in the dendrites, the functionally relevant regions of these synaptic proteins, and whether the dendritic fraction of PR is also altered by treatments. PR expression was observed in the nucleus, cell bodies, and along MAP2-postive dendrites (Figure 6A). E_2 increased both the nuclear and extra-nuclear PR expression in these neurones (Figure 6C). Despite the increase in nuclear expression, PR was predominately expressed in extra-nuclear locations, consistent with previous studies.[39,40,76] The E_2-induced increase in both nuclear and non-nuclear PR expression was not altered by co-treatment with either P4 or SKF. Similarly, PR antagonism with RU486 also had no effect on E_2-induced PR expression ($F_{5,93}$ =5.467, P = 0.0002, Tukey's post-hoc, one-way ANOVA; n = 12-20 cells from three independent hiPSC lines) (Figure 6B,C).

After confirming PR expression in the dendritic processes of these hiPSC neurones, we then investigated whether PR and SYN1/2 are co-expressed in dendrites to confirm the functional interactions of PR with these hypothalamic synaptic proteins. Indeed, dendrites positively labelled for both E_2-induced PR and SYN1/2 were detected for all E_2-treated conditions (Figure 7A). Taken together, these data demonstrate that these hiPSC-derived neurones are GnRH-positive and express E_2-induced PR, including in the SYN1/2-positive dendrites and thus serve as an appropriate cell model to test the effects of SKF on synapses mediated by E_2-induced PR.

3.8 | Dopaminergic D1R activation increases SYN1/2 expression in GnRH-positive hiPSC neurones in a PR-dependent manner

We have previously shown that activation of E_2-induced PR by P4 increases synaptic protein expression.[16] To determine whether SKF activation of PR can also regulate SYN1/2 expression, we examined their expression in D50 hiPSC neurones following treatment (Figure 7A). All neurones were treated with E_2 to induce PR expression. Interestingly, E_2 alone significantly increased SYN1/2 expression compared to the vehicle condition (Figure 7B). Moreover, co-treatment with E_2 and P4 induced a further increase in SYN1/2 expression compared to E_2 alone (Figure 7A,B). This was also mimicked by co-treatment with E_2 and SKF (Figure 7A,B). Critically, the effect of E_2 and SKF on SYN1/2 expression was attenuated by RU486, indicating the requirement of PR in mediating this effect ($F_{5,142}$ =29.34, P < 0.0001, Tukey's post-hoc, n = 15-34 cells from three independent hiPSC lines) (Figure 7B).

4 | DISCUSSION

In the absence of P4, DA activation of PR in rodent hypothalamus induces female reproductive behaviour.[33,50,54] In the present study, we tested the hypothesis that proteins from female mouse hypothalamus treated with SKF, a D1R agonist, interact with mouse PR in the absence of P4. Using pull-down assays, we identified many proteins from SKF-treated mouse hypothalami that interact with mouse PR-A, but not PR-B, in the absence of P4, suggesting that these proteins function in ligand-independent activation of PR-A. The majority of the DA-dependent PR-A interactome was comprised of synaptic proteins. To investigate the functional implications of these DA-dependent interactions of synaptic proteins with PR-A, hiPSC neurones that exhibit hypothalamic-like phenotype and express GnRH and E_2-induced PR were used to test PR-dependent effects on synaptic proteins. PR was co-expressed with SYN1/2 in the dendrites of hiPSC neurones, providing evidence for the functional interaction between the two proteins. Furthermore, we found that SYN1/2 expression is up-regulated in a PR-dependent manner. In these neurones, P4 increased SYN1/2 expression, confirming our previous findings that P4 functions in synaptic plasticity.[16] Moreover, in the absence of P4, DA activation of PR also increased SYN1/2 expression, which was blocked by the PR antagonist RU486, suggesting that this effect of SKF is PR-dependent. Taken together, the present findings suggest that DA activates hypothalamic PR via phosphorylation of proteins, such as DARPP-32[55] and facilitates the interaction of PR with additional neuronal proteins. The activated PR can further induce synaptic protein expression that could be

important in the regulation of brain function and behaviour. This ligand-independent activation of PR by SKF could mediate genomic or non-genomic changes.[33,50,54] Proteins that are integral in energy metabolism comprised the second largest functional group that complexed with PR-A in a DA-dependent manner, suggesting that PR-A functions in energy homeostasis. Furthermore, PR-A interacted with cytoskeletal proteins, ion channels, calcium sensors and cell signalling proteins, supporting a variety of important functions of PR-A in brain. Proteins required for DNA synthesis and protein synthesis, folding and transport also complexed with PR-A in a DA-dependent manner in the absence of P4, as demonstrated by MS analysis of hypothalamic proteins pulled-down using unliganded PR. In addition, proteins integral for posttranslational modifications (eg, phosphorylation, dephosphorylation and ubiquitination) interacted with mouse PR-A. The multiple proteins identified suggest that PR function can be regulated in a tissue- and context-specific manner depending on their binding partners and that the interaction of PR and DA systems affect multiple cellular processes, including metabolism and synaptic plasticity.

4.1 | DA-dependent interactions of hypothalamic synaptic proteins with PR-A

Progestins act via PR to strengthen synapse structure and function in rodent brain.[16,41-45,77] PR are expressed in dendritic spines and axon terminals in the hypothalamus and hippocampus of female rodents.[39,40,78] Moreover, PR activation increases dendritic spines and synapse density.[16,43] Synaptic vesicle-associated proteins identified in the present study, including syntaxin-1, SNAP25, synaptotagmin-1, SYN2, SYN3, VAMP1 and VAT1L, are important for vesicle docking and neurotransmitter release in a Ca^{2+}-dependent manner.[79,80] In particular, synapsins (eg, SYN2 and SYN3) are phosphoproteins essential for synapse formation, maturation, transmission and remodelling.[81,82] Our previous findings reveal that SYN1, SYN2 and SYN3 interact with PR in a P4-dependent manner.[16] Moreover, P4-induced synapse formation is dependent on SYN1 in rat primary cortical neurones.[16] Notably, an SKF-mediated increase in SYN1/2 expression in GnRH-positive hiPSC neurones suggests that PR alters synaptic plasticity by up-regulating synaptic proteins and facilitating their interactions with activated

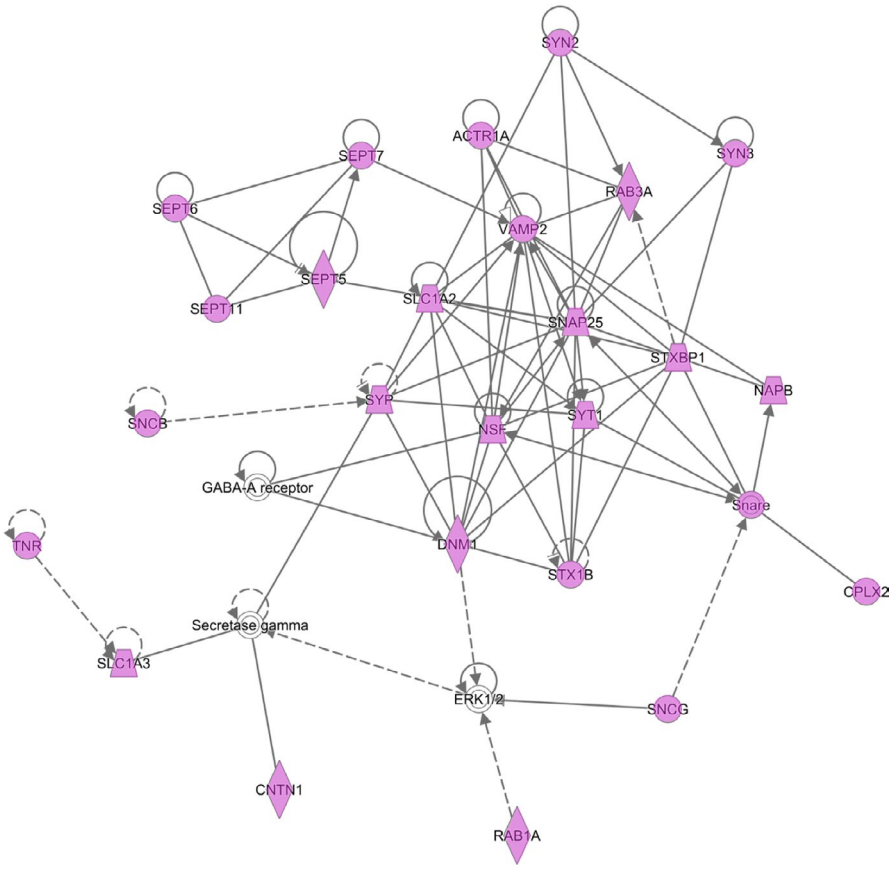

FIGURE 2 Ingenuity pathway analysis (IPA) network reveals hypothalamic synaptic proteins that associate with unliganded progestin receptor-A in an SKF-dependent manner. Proteins shaded in pink were identified in this study, whereas those in white were added to the network based on curated relationships in the IPA database. ___, direct interaction; ....., indirect interaction; ACTR1A, alpha-centractin; CNTN1, contactin-1; CPLX2, complexin-2; DNM1, dynamin-1; NAPB, beta-soluble NSF attachment protein; NSF, vesicle-fusing ATPase; RAB1A, Ras-related protein Rab-1A; RAB3A, Ras-related protein Rab-3A; SEPT (5, 6, 7,11), septin-(5, 6, 7, 11); SLC1A2, excitatory amino acid transporter 2; SLC1A3, excitatory amino acid transporter 1; SNAP25, synaptosomal-associated protein 25; SNCB, beta-synuclein; SNCG, gamma-synuclein; STX1B, syntaxin-1B; STXBP1, syntaxin-binding protein 1; SYN (2,3), synapsin (2, 3); SYP, synaptophysin; SYT1, synaptotagmin-1; TNR, tenascin-R; VAMP2, vesicle-associated membrane protein 2

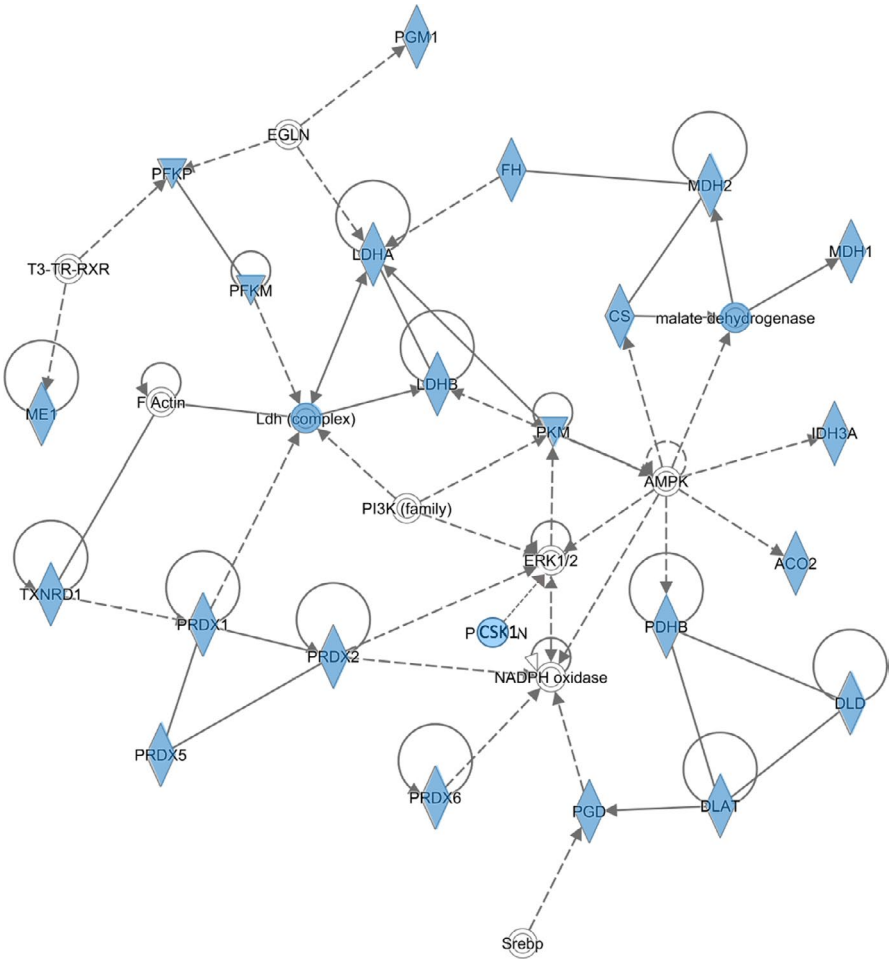

FIGURE 3 Ingenuity pathway analysis (IPA) network shows proteins involved in cellular and energy metabolism that associate with unliganded progestin receptor-A in an SKF-dependent manner. Proteins shaded in blue were identified in the present study, whereas those in white were added to the network based on curated relationships in the IPA database. ___, direct interaction; ....., indirect interaction; ACO2, aconitate hydratase, mitochondrial; AMPK, 5'-AMP-activated protein kinase; CS, citrate synthase; DLAT, dihydrolipoyllysine-residue acetyltransferase component of pyruvate dehydrogenase complex, mitochondrial; DLD, ddehydrogenase, mitochondrial; EGLN, Egl nine homologue; FH, fumarate hydratase; IDH3A, isocitrate dehydrogenase [NAD] subunit alpha, mitochondrial; LDH (A, B), L-lactate dehydrogenase (A, B); MDH1, malate dehydrogenase, cytoplasmic; MDH2, malate dehydrogenase, mitochondrial; ME1, NADP-dependent malic enzyme; PCSK1N, ProSAAS; PDHB, pyruvate dehydrogenase E1 component subunit beta, mitochondrial; PFKM, ATP-dependent 6-phosphofructokinase, muscle type; PFKP, ATP-dependent 6-phosphofructokinase, platelet type; PGD, 6-phosphogluconate dehydrogenase, decarboxylating; PGM1, phosphoglucomutase-1; PI3K, phosphatidylinositol 3-kinase; PKM, pyruvate kinase PKM; PRDX (1,2,5,6), peroxiredoxin (1,2,5,6); Srebp, sterol regulatory element-binding protein; T3-TR-RXR, T3-thyroid hormone receptor-retinoid-X receptor; TXNRD1, thioredoxin reductase 1, cytoplasmic

PR.[16,45] In the present study, additional synaptic proteins from SKF-treated brain that function in the synthesis, transport and clearance of neurotransmitters (EAA1, EAA2, AATC, DCE2, GLNA, GABT, SSDH, DHE3 and PCSK1) interacted with PR-A.[83-86] Taken together, these findings suggest that PR regulates synaptic physiology to elicit profound effects in brain function and behaviour.[14,18]

Phosphorylation of PR is an important step in DA-mediated PR activation of female reproductive behaviour in rodents.[33,49,54,87] Kinases, phosphatases and their substrates that were identified to interact with PR-A in the present study can directly act on synapses. In particular, DARPP-32, a substrate of D1R required for PR function,[85] was identified to associate with activated PR-A in the present study. DARPP-32 is expressed in PR-positive regions of the female hypothalamus [55,89,90] and is required for DA-mediated PR induction of reproductive behaviour in female rodents.[55,90] There was little to no SKF induction of sexual behaviour in mice treated with antisense to DARPP-32 and in DARPP32-KO mice.[55] DA-dependent sexual behaviour and SKF-mediated changes required for sexual receptivity were also blocked by the D1R antagonist SCH 23390, suggesting that D1R is required for SKF-mediated hypothalamic PR activation.[56,91] Although we did not detect D1R in the hypothalamic PR interactome, PR interacted with DARPP-32, an obligatory protein for DA-dependent PR activation and reproductive behaviour in female rodents.[55,89,90] Some phosphorylating partners, such as Src kinase from female mouse hypothalamus, interact with mouse PR-A, whereas activated human PR-B interacts with Src kinase in breast cells, suggesting tissue- and/or species-specific

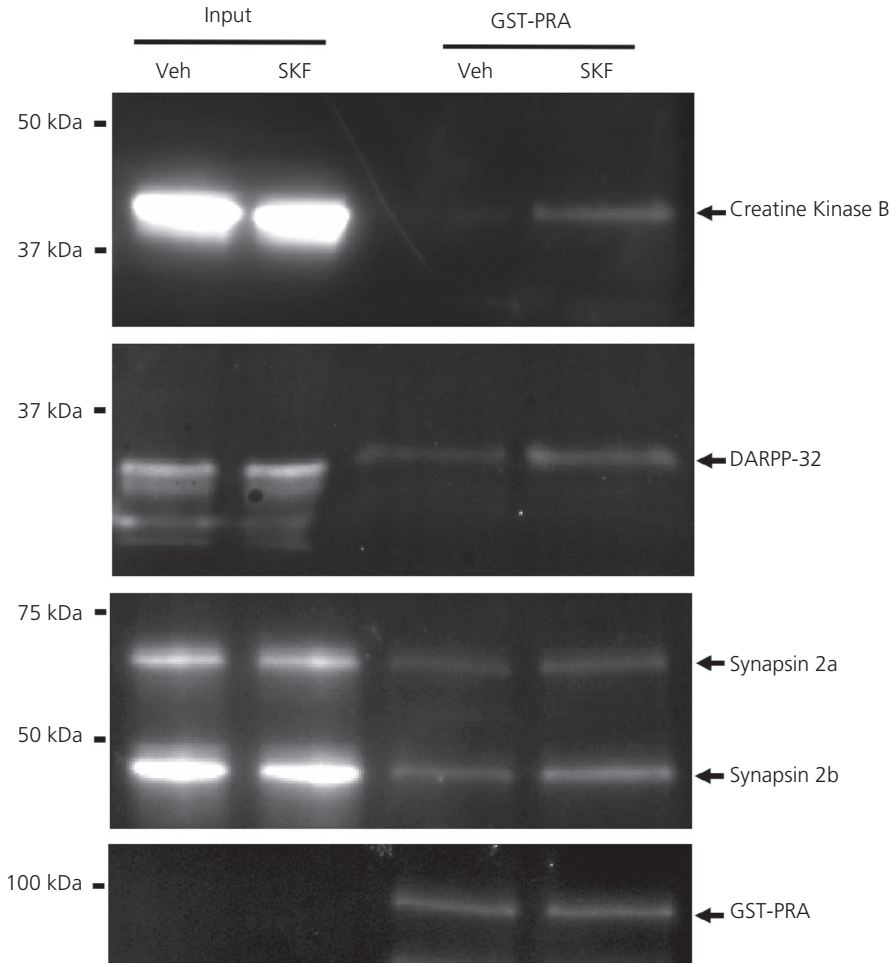

FIGURE 4 Hypothalamic proteins interact with mouse progestin receptor (PR)-A in an SKF-dependent manner. Western blots (n = 9 samples pooled per treatment condition) show that creatine kinase B, DARPP-32 and synapsin 2a and synapsin 2b from hypothalami treated with the D1 receptor (D1R) agonist SKF strongly associate with PR-A in the absence of progesterone compared to vehicle (Veh) samples. Input (0.25% of total) from hypothalamic extracts from Veh (lane 1) and SKF- (lane 2) treated mice. GST, glutathione *S*-transferase

interactions of the PR isoforms.[16,51] Taken together, the DA-dependent phosphorylation of DARPP-32 and other synaptic proteins are required for PR activation in the absence of P4.

Another enriched functional group in the DA-dependent PR-A interactome is the calcium signalling proteins. A tight regulation of Ca^{2+} influx is critical to synaptic physiology.[92] Excess Ca^{2+} influx can result in glutamate-induced excitatory damage, a common feature of traumatic brain injury (TBI) and other neurological disorders.[93] Progesterone provides neuroprotection in TBI,[2,3,94] by blocking calcium channels in synapses [95] and attenuating glutamate excitotoxicity.[86] The calcium regulators that are known to have protective effect against TBI, including calcineurin B1 [96] and calcium/calmodulin-dependent protein kinase type II (KCC2/CAMKII),[97] glutamate transporters EAA1 and EAA2, and glutamate-degrading enzymes GLNA and DHE3, all interacted with PR-A from SKF-treated hypothalamus, suggesting that PR-A activated by DA provides neuroprotection through Ca^{2+}-dependent regulation of synaptic glutamate levels. Excess Ca^{2+} accumulation can also compromise mitochondrial function and induce oxidative stress,[98] which is a hallmark of many neurodegenerative disorders.[99,100] Progestins improve mitochondrial functions, including ATP production and protection from oxidative damage in rat brain.[4] In the present study, the mitochondrial peroxiredoxins (PRDX1, PRDX2 and PRDX6) from SKF-treated hypothalamus associated with PR-A, suggesting that PR mediates neuroprotection against oxidative insults in a DA-dependent manner.

4.2 | PR-A interacts with energy metabolism-related hypothalamic proteins in a DA-dependent manner

Progestins regulate energy homeostasis in women, non-human primates and rodents.[16,101-104] In support, PR are expressed in adipocytes and muscles and P4 increases glycogen breakdown and decreases glucose transport to muscles.[105,106] Isoform-specific interaction assays showed that PR-A, but not PR-B, associates with hypothalamic metabolic regulators when activated by P4.[16] In the present study, several key metabolic mediators (eg, regulators of glycolysis, TCA cycle, glycogen utilisation and oxidative phosphorylation) associated with PR-A in a DA-dependent manner, strongly supporting a role for PR in energy metabolism in the hypothalamus. For example, creatine kinase B, a major catalyser of ATP production in brain, complexed with PR-A, but not PR-B, in the presence of P4 [16] or in the absence of P4 in a DA-dependent manner, as confirmed by MS and western blotting. Consistent with P4-dependent activation in rat skeletal muscle,[106] we identified an increased interaction with PR-A of a rate limiting enzyme for glycogenolysis, PYGB from SKF-treated brain, suggesting that DA activation of PR-A increases energy availability to neurones. PR can also alter energy metabolism in non-neuronal tissues. Elevated levels of PR in breast tumours in obese rats correlate with increased expression of proteins involved in carbohydrate and lipid metabolism, including glycolysis (G6PI and

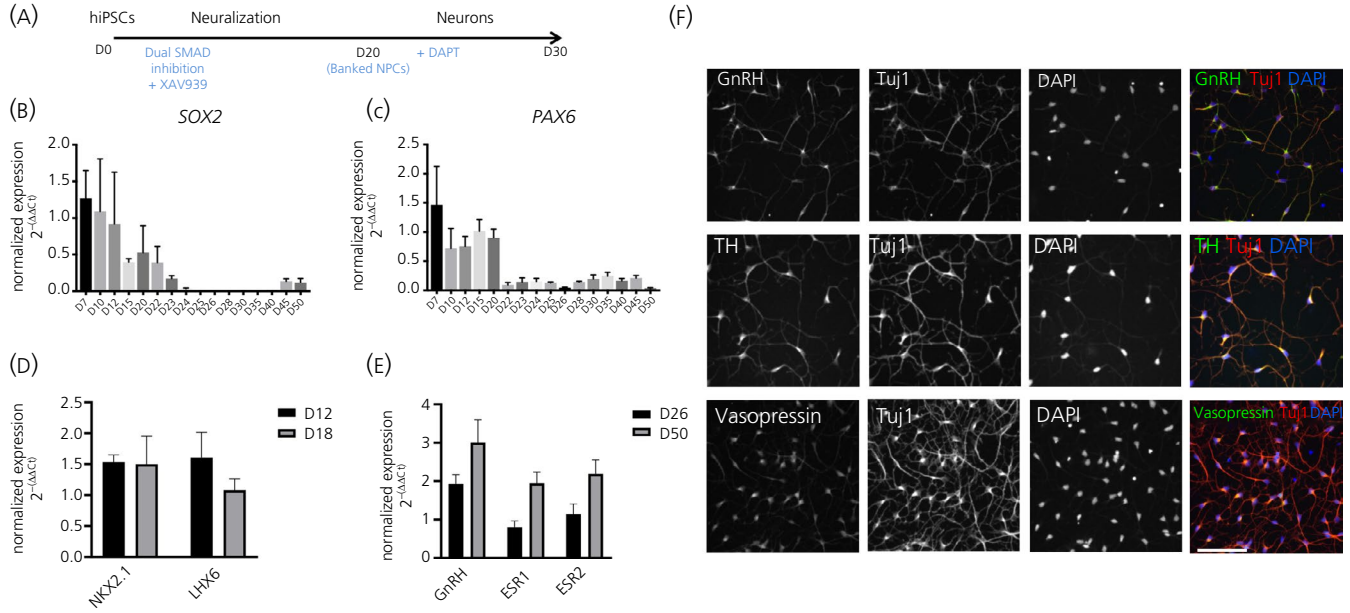

FIGURE 5 Generation of gonadotrophin-releasing hormone (GnRH)-positive hypothalamic-like neurones (human-induced pluripotent stem cell [hiPSC] neurones). (A) Schematic of hiPSC differentiation protocol used. (B and C) Expression profile of cell fate markers determined between day 7 (D7) and D50 following induction of neural differentiation; error bars represent the SD. Neuroepithelial marker *SOX2* (B) and forebrain marker *PAX6* (C) are both highly expressed from D7 to D20, although their expressions is greatly reduced thereafter. (D) Expression levels of *NKX2.1* and *LHX6*, markers of hypothalamic-like identity were highly expressed in D12 and D18 neural progenitor cells (NPCs); error bars represent the SEM. (E) Assessment of mRNA levels in immature (D26) and developing (D50) neurones revealed an increase in expression levels for *GnRH*, as well as oestrogen receptors *ESR1* and *ESR2*; error bars represent the SEM. (F) Representative images of hiPSC neurones (D26) immunostained for markers of specific cell fate. This revealed that D26 immature hiPSC neurones were positive for the neural marker Tuj1, GnRH, tyrosine hydroxylase (TH) and vasopressin. DAPI, 4',6-diamidino-2-phenylindole. Scale bar = 100 μm

G3P), TCA cycle (IDH3A and PGK1) and glycogen utilisation (PYGB and PGM1),[107] which all associated with PR-A following DA activation in the present study. The present findings extend these previous studies in breast tumours to suggest that DA-activated PR (in the absence of P4) contributes to the metabolic functions of PR in brain. The identification of these PR-dependent pathways that are mediated by DA and conserved in brain and breast tumours could enable the development of common therapeutic targets for these tissues.

Because synaptic proteins were previously identified as the largest functional group that interact with P4-activated PR,[16] in the present study, we aimed to determine whether the synaptic proteins also function in ligand-independent PR activation. In particular, SYN1/2, the synaptic proteins that complexed with PR in both ligand-bound and unliganded conditions are increased along dendrites of hiPSC neurones following DA-dependent PR activation. This increase was blocked by RU486, suggesting that this effect is PR-specific. Furthermore, i.c.v. administration of SKF 30 minutes prior to tissue collection increased SYN1/2 expression compared to the E_2-treated group. This SKF-induced increase in dendritic SYN1/2 was also effectively blocked by the PR antagonist RU486, suggesting that the effect is PR-dependent. Although RU486 can inhibit both transcriptional activity of PR [108] and block the SKF-dependent PR facilitation of reproductive behaviour in female rodents,[109] our present data are limited with respect to providing specific mechanisms by which SKF increases, and RU486 inhibits, this PR-mediated SYN1/2 expression. Taken together, these data suggest that PR can affect expression of proteins regulating synaptic function in both the ligand-dependent and -independent manner.

Interestingly, there was a lack of interaction of PR-B with proteins from SKF-treated hypothalamus. It is possible that the PR-B-interactome signals were not sufficiently strong to be detected by MS. In addition, it should be noted that the mouse PR-B used in the present pull-down assays was not endogenously expressed in mouse hypothalamus; however, Sf9 insect cells are a well-established system for the expression of tagged proteins, including GST-PR A and GST-PR B.[16,110] In support of the present findings, a dominant role for ligand-dependent or ligand-independent activation of PR-A over PR-B has been reported in brain, breast and ovarian tissue.[111,112]

4.3 | GnRH-positive hiPSC neurones as an in vitro model for the study of PR function in synapses

In the present study, GnRH-positive hiPSC neurones are provided as a suitable in vitro model for investigating the DA-dependent effects of PR in synapses. These neurones exhibit E_2 and P4-dependent regulation of GnRH expression and function.[66-71] PR are co-expressed with SYN1/2 in these neuronal processes, providing evidence for the significance of the interactions detected

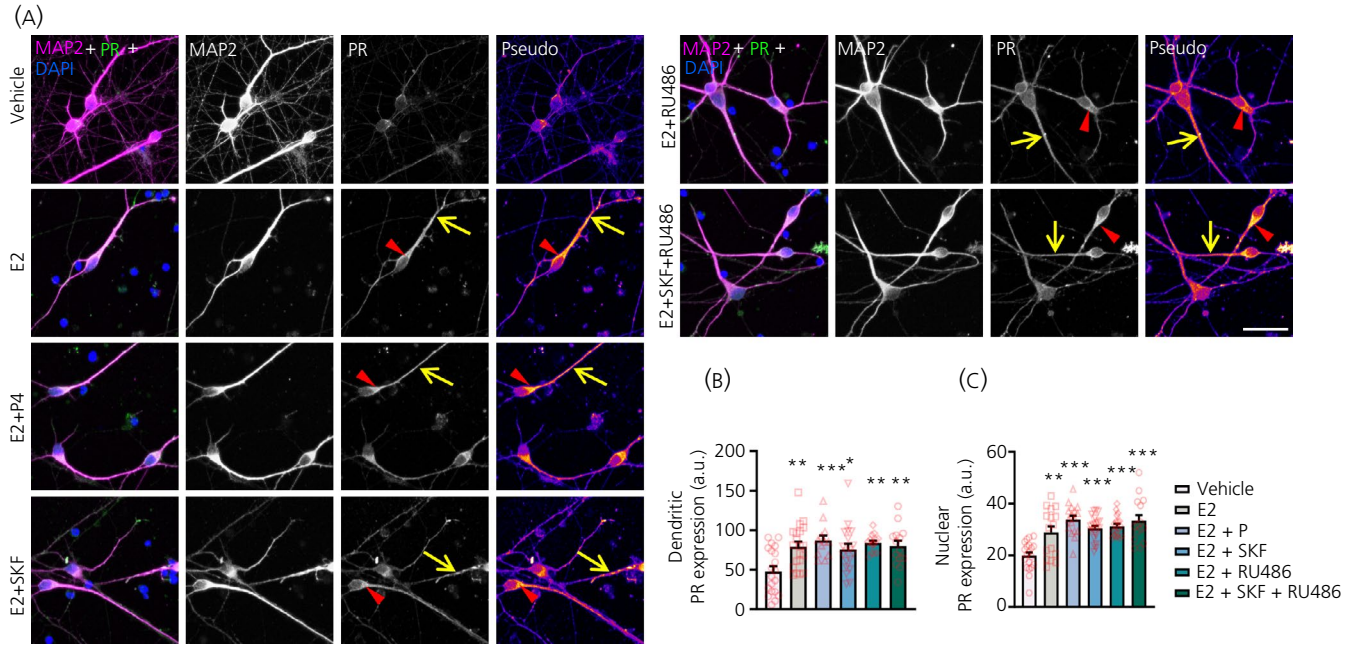

FIGURE 6 Induction of progestin receptor (PR) expression by 17β-oestradiol (E_2) in gonadotrophin-releasing hormone-positive human-induced pluripotent stem cell (hiPSC) neurones. (A) Representative confocal images of day (D)50 hiPSC neurones immunostained for MAP2 (morphological marker) and PR; 4',6-diamidino-2-phenylindole (DAPI) was used to identify nuclei of cells. hiPSC-GnRH-neurones from three hiPSC-lines were neutralised and subsequently treated with 10 nM 17β-oestradiol (E_2), 1 nM progesterone (P4) or 10 nM RU486 for 24 hours. For the groups that received SKF38393 (SKF; D1-dopamine receptor agonist), a 30-minute incubation with SKF followed 24 hours of the respective hormone treatment. Red arrowheads indicate PR expression within the cell body; yellow arrows indicate elevated PR expression along MAP2-positive neurites. Psuedo images refer to PR abundance: darker colours indicate lower expression, whereas red/yellow psuedocolouring indicates increased abundance. Scale bar = 10 μm. (B) Quantification of PR expression along MAP2-positive dendrites. (C) Quantification of nuclear PR expression. Error bars represent the SEM and symbols display data points from individual cells analysed; n = 12-20 cell from three independent hiPSC lines. (* $P < 0.05$, ** $P < 0.01$, *** $P < 0.001$; compared to vehicle; one-way ANOVA with Tukey's post-hoc correction)

via pull-down assays. Furthermore, SKF up-regulated SYN1/2 in a PR-dependent manner in these neurones, suggesting that these neurones are an appropriate in vitro model for studying ligand-independent activation of PR.

However, it should be noted that there are substantial differences between these hiPSC-derived neurones and rodent GnRH neurones found in the hypothalamus. GnRH neurones originate outside the hypothalamus from a subset of neural progenitors found within the olfactory placode, which subsequently migrate into the hypothalamus. There is also evidence that GnRH neurones may descend from neural crest progenitors.[113] The differentiation protocol used in the present study best recapitulates the generation of GnRH neurones from placode progenitors.[114,115] In humans, GnRH neurones that emerge from the olfactory placode migrate to the hypothalamus, as well as other brain regions.[116] It is possible that we have modelled the effects of E_2 and P4 on GnRH neurones that are found outside of the hypothalamus. Based on RNA sequencing studies, the GnRH-positive hiPSC neurones express a number of genes that have not been previously described in GnRH neurones from animal models[117] but, instead, best resemble human fetal GnRH neurones. These differences could explain the disparities between the present study and those from GnRH neurones in adult rodents.[117]

5 | CONCLUSIONS AND FUTURE DIRECTIONS

An enhanced representation of synaptic proteins and metabolic regulators in the ligand-independent PR interactome provides novel mechanisms for activation of PR by DA in the brain. In particular, DA-dependent interactions of hypothalamic proteins with PR-A, but not PR-B, is supported by previous findings indicating that PR-A exerts a dominant role in ligand-independent activation by DA with respect to inducing female reproductive behaviour.[33] Using physiologically relevant brain tissue, the present study identified novel interactions of DA-activated hypothalamic proteins, including a large set of synaptic proteins, with PR-A in the absence of P4. Although pull-down assays are a powerful approach for investigating protein-protein interactions in vitro as a result of their high sensitivity, it will be important for future studies to confirm the present findings using co-immunoprecipitation to identify hypothalamic PR-protein interactions in vivo and to investigate the direct functional outcomes of these interactions in brain function and behaviour. Using a cell model of GnRH-positive hypothalamic-like neurones derived from hiPSCs that contain E_2-induced PR, we found that DA activation of PR up-regulates proteins important for synaptic plasticity. Notably, no interactions of hypothalamic

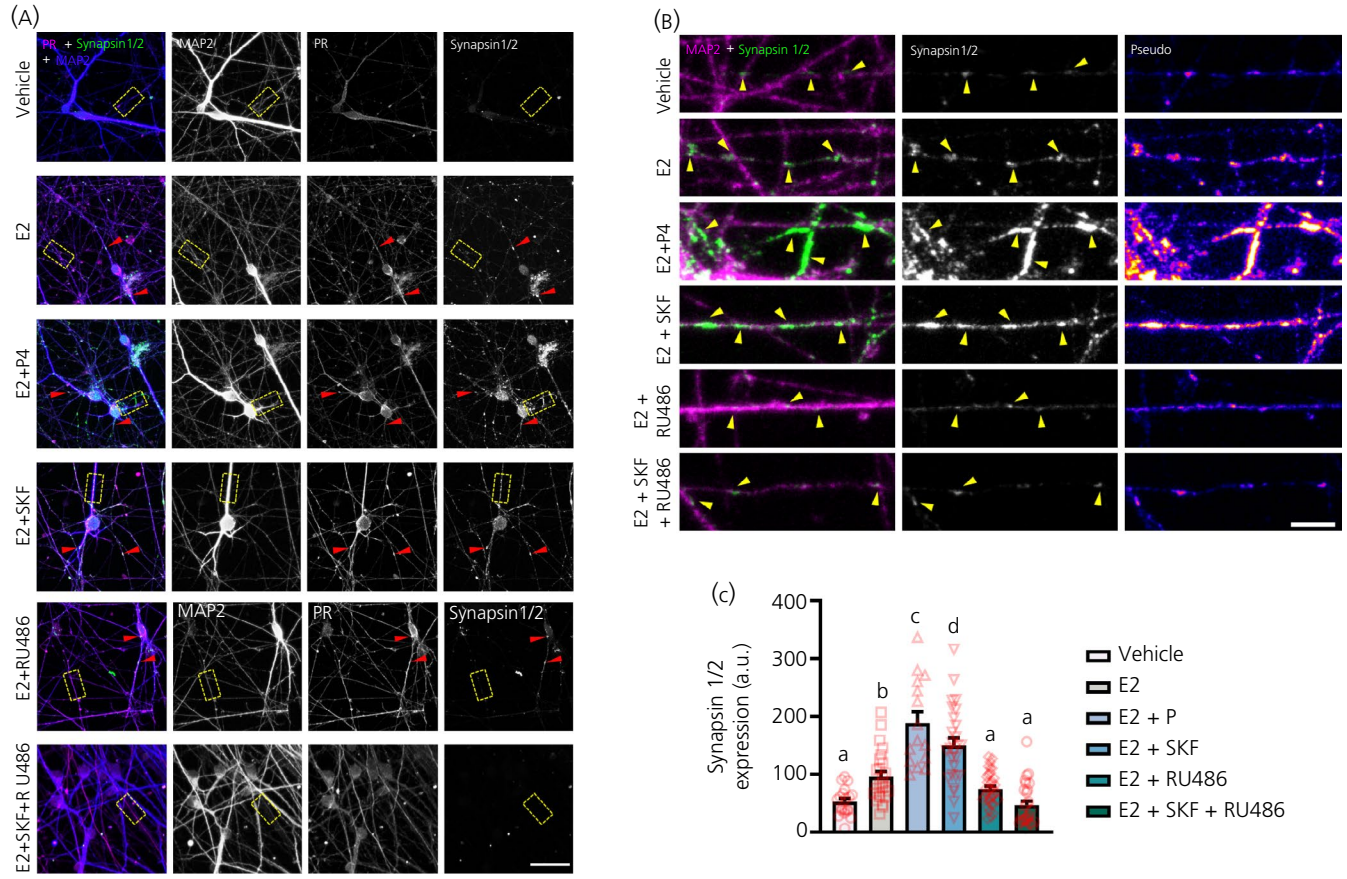

FIGURE 7 Regulation of synapsin1/2 expression by D1 receptor activation in gonadotrophin-releasing hormone (GnRH)-positive human-induced pluripotent stem cell (hiPSC) neurones. (A) Representative confocal images of cells co-stained for MAP2 (blue), progestin receptor (PR) (magenta) and synapsin1/2 (green). Neurones were treated with 10 nmol L^{-1} 17β-oestradiol (E_2), 1 nmol L^{-1} progesterone (P4) or 10 nmol L^{-1} RU486 for 24 hours. For the groups that received SKF (D1-receptor agonist), a 30-minute incubation with SKF followed 24 hours of the respective hormone treatment. PR and synapsin 1/2 expression can be seen in the same cell, including along MAP2-positive dendrites of day 50 hiPSC neurones. Dashed yellow rectangles show regions magnified in (B). Scale bar = 10 μm. (B) Yellow arrowheads indicate synapsin 1/2 expression along MAP2-positive neurites. Psuedo images refer to synapsin 1/2 abundance: darker colours indicate lower expression, whereas red/yellow psuedocolouring indicates increased abundance. Scale bar = 5 μm. (C) Quantification of synapsin 1/2 expression along MAP2-positive dendrites following treatments. Error bars represent the SEM and symbols display data points from individual cells analysed; n = 15-34 cells from three independent hiPSC lines (different lowercase letters denote differences among groups; one-way ANOVA with Tukey's post-hoc correction)

D1R with PR, regardless of SKF treatment, were detected. To determine whether DA can act directly on PR in neurones, it will be important in future studies to investigate whether D1R and PR are co-expressed in mouse PR-expressing hypothalamic and extra-hypothalamic regions, such as the ventral tegmental area,[118] posterodorsal medial nucleus of the amygdala[91] and cortex.[119] The present PR-protein interaction findings also suggest important functions of PR-A in metabolic homeostasis. These novel findings of protein complexes involved in the DA activation of PR in the absence of hormone provide potential candidates for therapeutic targets with respect to a variety of disorders of reproduction, mental health and metabolism in women.

ACKNOWLEDGEMENTS

This work was funded by NIH R01 DK61935 (MJT), NIH 5U24DK076169-13 (RM) Subaward # 30835-64 (KDA), and the European Union's Seventh Framework Programme for research, technological development and demonstration under grant agreement no 603016 (DPS). We thank the Wohl Cellular Imaging Centre (WCIC) at the IoPPN, Kings College London, for help with microscopy and the staff of the Mass Spectrometry Facility (MSF) at University of Texas Medical Branch for guidance on sample preparation, LCMS analysis, and informatics of the proteomic samples.

DATA AVAILABILITY

The data that support the findings of the present study are available from the corresponding author upon reasonable request.

ORCID

Kalpana D. Acharya https://orcid.org/0000-0001-6263-4357
Deepak P. Srivastava https://orcid.org/0000-0001-6512-9065

Marc J. Tetel https://orcid.org/0000-0002-9843-4071

REFERENCES

1. Wei J, Xiao GM. The neuroprotective effects of progesterone on traumatic brain injury: current status and future prospects. *Acta Pharmacol Sin*. 2013;34:1485-1490.
2. Stein DG, Hoffman SW. Estrogen and progesterone as neuroprotective agents in the treatment of acute brain injuries. *Pediatr Rehabil*. 2003;6:13-22.
3. Singh M. P-mediated neuroprotection. *Endocrine*. 2006;29:271-274.
4. Irwin RW, Yao J, Hamilton RT, Cadenas E, Brinton RD, Nilsen J. Progesterone and estrogen regulate oxidative metabolism in brain mitochondria. *Endocrinology*. 2008;149:3167-3175.
5. Su C, Cunningham RL, Rybalchenko N, Singh M. Progesterone increases the release of brain-derived neurotrophic factor from glia via progesterone receptor membrane component 1 (Pgrmc1)-dependent ERK5 signaling. *Endocrinology*. 2012;153:4389-4400.
6. Hull EM, Franz JR, Snyder AM, Nishita JK. Perinatal progesterone and learning, social and reproductive behavior in rats. *Physiol Behav*. 1980;24:251-256.
7. Sandstrom NJ, Williams CL. Memory retention is modulated by acute estradiol and progesterone replacement. *Behav Neurosci*. 2001;115:384-393.
8. Wagner CK. The many faces of progesterone: a role in adult and developing male brain. *Front Neuroendocrinol*. 2006;27:340-359.
9. Mora S, Dussaubat N, Díaz-Véliz G. Effects of the estrous cycle and ovarian hormones on behavioral indices of anxiety in female rats. *Psychoneuroendocrinology*. 1996;21:609-620.
10. Blaustein JD, Ismail N. Enduring influence of pubertal stressors on behavioral response to hormones in female mice. *Horm. Behav*. 2013;64:390-398.
11. Keyes KM, Cheslack-Postava K, Westhoff C, et al. Association of hormonal contraceptive use with reduced levels of depressive symptoms: A national study of sexually active women in the United States. *Am J Epidemiol*. 2013;178:1378-1388.
12. Uphouse L, Adams S, Miryala CS, Hassell J, Hiegel C. RU486 blocks effects of allopregnanolone on the response to restraint stress. *Pharmacol Biochem Behav*. 2013;103:568-572.
13. Lydon JP, DeMayo FJ, Funk CR, et al. Mice lacking progesterone receptor exhibit pleiotropic reproductive abnormalities. *Genes Dev*. 1995;9:2266-2278.
14. Mani SK, Blaustein JD. Neural progestin receptors and female sexual behavior. *Neuroendocrinology*. 2012;96:152-161.
15. Sinchak K, Micevych PE. Progesterone Blockade of Estrogen Activation of μ-Opioid Receptors Regulates Reproductive Behavior. *J Neurosci*. 2001;21:5723-5729.
16. Acharya KD, Nettles SA, Sellers KJ, et al. The Progestin Receptor Interactome in the Female Mouse Hypothalamus: Interactions with Synaptic Proteins Are Isoform-Specific and Ligand-Dependent. *eNeuro*. 2017;4:1-19.
17. Acharya KD, Finkelstein SD, Bless EP, et al. Estradiol preferentially induces progestin receptor-A (PR-A) over PR-B in cells expressing nuclear receptor coactivators in the female mouse hypothalamus. *eNeuro*. 2015;2:12-15.
18. Tetel MJ, Lange CA. *Molecular Genomics of Progestin Actions*. San Diego, CA: Academic Press 2009:1439-1465.
19. Intlekofer KA, Petersen SL. 17β-estradiol and progesterone regulate multiple progestin signaling molecules in the anteroventral periventricular nucleus, ventromedial nucleus and sexually dimorphic nucleus of the preoptic area in female rats. *Neuroscience*. 2011;176:86-92.
20. Kastner P, Krust A, Turcotte B, et al. Two distinct estrogen-regulated promoters generate transcripts encoding the two functionally different human progesterone receptor forms A and B. *EMBO J*. 1990;9:1603-1614.
21. Lessey BA, Alexander PS, Horwitz KB. The subunit structure of human breast cancer progesterone receptors: characterization by chromatography and photoaffinity labeling. *Endocrinology*. 1983;112:1267-1274.
22. Schott DR, Shyamala G, Schneider W, Parry G. Molecular cloning, sequence analyses, and expression of complementary DNA encoding murine progesterone receptor. *Biochemistry*. 1991;30:7014-7020.
23. Horwitz KB, Sheridan PL, Wei LL, Krett NL. Human progesterone receptors: synthesis, structure, and phosphorylation. *Prog Clin Biol Res*. 1990;322:41-52.
24. Hovland AR, Powell RL, Takimoto GS, Tung L, Horwitz KB. An N-terminal inhibitory function, IF, suppresses transcription by the A-isoform but not the B-isoform of human progesterone receptors. *J Biol Chem*. 1998;273:5455-5460.
25. Kraus WL, Montano MM, Katzenellenbogen BS. Identification of multiple, widely spaced estrogen-responsive regions in the rat progesterone receptor gene. *Mol Endocrinol*. 1994;8:952-969.
26. Stanisic V, Lonard DM, O'Malley BW. Modulation of steroid hormone receptor activity. *Prog Brain Res*. 2010;181:153-176.
27. Sartorius CA, Melville MY, Hovland AR, Tung LT, Takimoto GS, Horwitz KB. A third transactivation function (AF3) of human progesterone receptors located in the unique N-terminal segment of the B-isoform. *Mol Endocrinol*. 1994;8:1347-1360.
28. Giangrande PH, Pollio G, McDonnell DP. Mapping and characterization of the functional domains responsible for the differential activity of the A and B isoforms of the human progesterone receptor. *J Biol Chem*. 1997;272:32889-32900.
29. Conneely OM, Lydon JP, De Mayo F, O'Malley BW. Reproductive functions of the progesterone receptor. *J Soc Gynecol Investig*. 2000;7(1 Suppl):S25-32.
30. Cheng KW, Cheng CK, Leung PC. Differential role of PR-A and -B isoforms in transcription regulation of human GnRH receptor gene. *Mol Endocrinol*. 2001;15:2078-2092.
31. Richer JK, Jacobsen BM, Manning NG, Abel MG, Wolf DM, Horwitz KB. Differential gene regulation by the two progesterone receptor isoforms in human breast cancer cells. *J Biol Chem*. 2002;277:5209-5218.
32. Mulac-Jericevic B, Lydon JP, DeMayo FJ, Conneely OM. Defective mammary gland morphogenesis in mice lacking the progesterone receptor B isoform. *Proc Natl Acad Sci USA*. 2003;100:9744-9749.
33. Mani SK, Reyna AM, Chen JZ, Mulac-Jericevic B, Conneely OM. Differential Response of Progesterone Receptor Isoforms in Hormone-Dependent and -Independent Facilitation of Female Sexual Receptivity. *Mol Endocrinol*. 2006;20:1322-1332.
34. Conneely OM, Mulac-Jericevic B, Lydon JP, De Mayo FJ. Reproductive functions of the progesterone receptor isoforms: lessons from knock-out mice. *Mol Cel Endocrinol*. 2001;179:97-103.
35. Conneely OM, Mulac-Jericevic B, Lydon JP. Progesterone-dependent regulation of female reproductive activity by two distinct progesterone receptor isoforms. *Steroids*. 2003;68:771-778.
36. Apostolakis EM, Ramamurphy M, Zhou D, Oñate S, O'Malley BW. Acute disruption of select steroid receptor coactivators prevents reproductive behavior in rats and unmasks genetic adaptation in knockout mice. *Mol Endocrinol*. 2002;16:1511-1523.
37. Molenda-Figueria HA, Griffin AL, Auger AP, McCarthy MM, Tetel MJ. Nuclear receptor coactivators modulate hormone-dependent gene expression in brain and female reproductive behavior in rats. *Endocrinology*. 2002;143:436-444.
38. Molenda-Figueira HA, Williams CA, Griffin AL, Rutledge EM, Blaustein JD, Tetel MJ. Nuclear receptor coactivators function in

estrogen receptor- and progestin receptor-dependent aspects of sexual behavior in female rats. *Horm Behav*. 2006;50:383-392.
39. Waters EM, Torres-Reveron A, McEwen BS, Milner TA. Ultrastructural localization of extranuclear progestin receptors in the rat hippocampal formation. *J Comp Neurol*. 2008;511:34-46.
40. Mitterling KL, Spencer JL, Dziedzic N, et al. Cellular and subcellular localization of estrogen and progestin receptor immunoreactivities in the mouse hippocampus. *J Comp Neurol*. 2010;518:2729-2743.
41. Woolley CS, McEwen BS. Roles of estradiol and progesterone in regulation of hippocampal dendritic spine density during the estrous cycle in the rat. *J Comp Neurol*. 1993;336:293-306.
42. McEwen BS, Woolley CS. Estradiol and progesterone regulate neuronal structure and synaptic connectivity in adult as well as developing brain. *Exp Gerontol*. 1994;29:431-436.
43. Chen JR, Yan YT, Wang TJ, Chen LJ, Wang YJ, Tseng GF. Gonadal hormones modulate the dendritic spine densities of primary cortical pyramidal neurons in adult female rat. *Cereb Cortex*. 2009;19:2719-2727.
44. Sanchez AM, Flamini MI, Genazzani AR, Simoncini T. Effects of Progesterone and Medroxyprogesterone on actin remodeling and neuronal spine formation. *Mol Endocrinol*. 2013;27:693-702.
45. Griffin GD, Ferri-Kolwicz SL, Reyes BA, Van Bockstaele EJ, Flanagan-Cato LM. Ovarian hormone-induced reorganization of oxytocin-labeled dendrites and synapses lateral to the hypothalamic ventromedial nucleus in female rats. *J Comp Neurol*. 2010;518:4531-4545.
46. Kyo S, Sakaguchi J, Kiyono T, et al. Forkhead transcription factor FOXO1 is a direct target of progestin to inhibit endometrial epithelial cell growth. *Clin Cancer Res*. 2011;17:525-537.
47. Pfaff DW, Schwartz-Giblin S, McCarthy MM, Kow LM. Cellular and molecular mechanisms of female reproductive behaviors. In: Knobil E, Neill JD, eds. *The Physiology of Reproduction*, vol. 77. New York: Raven Press; 1994:107-220.
48. Beyer C, Gonzalez-Flores O, Garcia-Juarez M, Gonzalez-Mariscal G. Non-ligand activation of estrous behavior in rodents: cross-talk at the progesterone receptor. *Scand J Psychol*. 2003;44:221-229.
49. Power RF, Mani SK, Codina J, Conneely OM, O'Malley BW. Dopaminergic and ligand-independent activation of steroid hormone receptors. *Science*. 1991;254:1636-1639.
50. Mani S, Allen J, Clark J, Blaustein J, O'Malley B. Convergent pathways for steroid hormone- and neurotransmitter-induced rat sexual behavior. *Science*. 1994;265:1246-1249.
51. Boonyaratanakornkit V, Scott MP, Ribon V, et al. Progesterone receptor contains a proline-rich motif that directly interacts with SH3 domains and activates c-Src family tyrosine kinases. *Mol Cell*. 2001;8:269-280.
52. Migliaccio A, Piccolo D, Castoria G, et al. Activation of the Src/p21ras/Erk pathway by progesterone receptor via cross-talk with estrogen receptor. *EMBO*. 1998;17:2008-2018.
53. Lange CA, Shen T, Horwitz KB. Phosphorylation of human progesterone receptors at serine-294 by mitogen-activated protein kinase signals their degradation by the 26S proteasome. *Proc Natl Acad Sci USA*. 2000;97:1032-1037.
54. Mani SK, Allen JM, Lydon JP, et al. Dopamine requires the unoccupied progesterone receptor to induce sexual behavior in mice. *Mol Endocrinol*. 1996;10:1728-1737.
55. Mani SK, Fienberg AA, O'Callaghan JP, et al. Requirement for DARPP-32 in Progesterone-Facilitated Sexual Receptivity in Female Rats and Mice. *Science*. 2000;287:1053-1056.
56. Mani S. Ligand-independent activation of progestin receptors in sexual receptivity. *Horm Behav*. 2001;40:183-190.
57. Paxinos G , Franklin KBJ. *The mouse brain in stereotaxic coordinate*. Compact 2nd ed. Amsterdam, The Netherlands: Elsevier Academic Press; 2004. http://www.loc.gov/catdir/description/els041/2003113435.html
58. Tetel MJ, Giangrande PH, Leonhardt SA, McDonnell DP, Edwards DP. Hormone-Dependent Interaction between the Amino- and Carboxyl- Terminal Domains of Progesterone Receptor in Vitro and in Vivo. *Endocrinology*. 1999;13:910-924.
59. Oberg AL, Vitek O. Statistical design of quantitative mass spectrometry-based proteomic experiments. *J Proteome Res*. 2009;8:2144-2156.
60. Eng JK, McCormack AL, Yates JR. An approach to correlate tandem mass spectral data of peptides with amino acid sequences in a protein database. *J Am Soc Mass Spectrom*. 1994;5:976–989.
61. MacLean B, Tomazela DM, Shulman N, et al. Skyline: an open source document editor for creating and analyzing targeted proteomics experiments. *Bioinformatics*. 2010;26:966-968.
62. Schilling B, Rardin MJ, MacLean BX, et al. Platform-independent and label-free quantitation of proteomic data using MS1 extracted ion chromatograms in skyline: application to protein acetylation and phosphorylation. *Mol Cell Proteomics*. 2012;11:202-214.
63. Cocks G, Curran S, Gami P, et al. The utility of patient specific induced pluripotent stem cells for the modelling of Autistic Spectrum Disorders. *Psychopharmacology*. 2014;231:1079-1088.
64. Deans PJM, Raval P, Sellers KJ, et al. Psychosis Risk Candidate ZNF804A Localizes to Synapses and Regulates Neurite Formation and Dendritic Spine Structure. *Biol Psychiatry*. 2017;82:49-61.
65. Kathuria A, Nowosiad P, Jagasia R, et al. Stem cell-derived neurons from autistic individuals with SHANK3 mutation show morphogenetic abnormalities during early development. *Mol Psychiatry*. 2018;23:735-746.
66. Shum C, Macedo SC, Warre-Cornish K, Cocks G, Price J, Srivastava DP. Utilizing induced pluripotent stem cells (iPSCs) to understand the actions of estrogens in human neurons. *Horm Behav*. 2015;74:228-242.
67. Shi Y, Kirwan P, Smith J, Robinson HP, Livesey FJ. Human cerebral cortex development from pluripotent stem cells to functional excitatory synapses. *Nat Neurosci*. 2012;15:477-486.
68. D'Agostino RB, Belanger A. A suggestion for using powerful and informative tests of normality. *The American Statistician*. 1990;44:316–321.
69. Bashour NM, Wray S. Progesterone directly and rapidly inhibits GnRH neuronal activity via progesterone receptor membrane component 1. *Endocrinology*. 2012;153:4457-4469.
70. He W, Li X, Adekunbi D, et al. Hypothalamic effects of progesterone on regulation of the pulsatile and surge release of luteinising hormone in female rats. *Sci Rep*. 2017;7:8096.
71. Ng Y, Wolfe A, Novaira HJ, Radovick S. Estrogen regulation of gene expression in GnRH neurons. *Mol Cell Endocrinol*. 2009;303:25-33.
72. Merkle FT, Maroof A, Wataya T, et al. Generation of neuropeptidergic hypothalamic neurons from human pluripotent stem cells. *Development*. 2015;142:633-643.
73. Wang L, Meece K, Williams DJ, et al. Differentiation of hypothalamic-like neurons from human pluripotent stem cells. *J Clin Invest*. 2015;125:796-808.
74. Xie Y, Dorsky RI. Development of the hypothalamus: conservation, modification and innovation. *Development*. 2017;144:1588-1599.
75. Shimogori T, Lee DA, Miranda-Angulo A, et al. A genomic atlas of mouse hypothalamic development. *Nat Neurosci*. 2010;13:767-775.
76. Milner TA, Mitterling KL, Iadecola C, Waters EM. Ultrastructural localization of extranuclear progestin receptors relative to C1 neurons in the rostral ventrolateral medulla. *Neurosci Lett*. 2008;431:167-172.
77. Chisholm NC, Juraska JM. Effects of long-term treatment with estrogen and medroxyprogesterone acetate on synapse number in the medial prefrontal cortex of aged female rats. *Menopause*. 2012;19:804-811.

78. Blaustein JD, King JC, Toft DO, Turcotte J. Immunocytochemical localization of estrogen-induced progestin receptors in guinea pig brain. *Brain Res*. 1988;474:1-15.
79. Pang ZP, Shin OH, Meyer AC, Rosenmund C, Sudhof TC. A gain-of-function mutation in synaptotagmin-1 reveals a critical role of Ca2+-dependent soluble N-ethylmaleimide-sensitive factor attachment protein receptor complex binding in synaptic exocytosis. *J Neurosci*. 2006;26:12556-12565.
80. Sudhof TC, Rizo J. Synaptic vesicle exocytosis. *Cold Spring Harb Perspect Biol*. 2011;3:a005637.
81. Ferreira A, Chin LS, Li L, Lanier LM, Kosik KS, Greengard P. Distinct roles of synapsin I and synapsin II during neuronal development. *Mol Med*. 1998;4:22-28.
82. Bogen IL, Jensen V, Hvalby O, Walaas SI. Synapsin-dependent development of glutamatergic synaptic vesicles and presynaptic plasticity in postnatal mouse brain. *Neuroscience*. 2009;158:231-241.
83. Maragakis NJ, Dietrich J, Wong V, et al. Glutamate transporter expression and function in human glial progenitors. *Glia*. 2004;45:133-143.
84. Erlander MG, Tobin AJ. The Structural and Functional Heterogeneity of Glutamic Acid Decarboxylase: A Review. *Neurochem Res*. 1991;16:215-226.
85. Gibson KM, Hoffmann GF, Hodson AK, Bottiglieri T, Jakobs C. 4-Hydroxybutyric acid and the clinical phenotype of succinic semialdehyde dehydrogenase deficiency, an inborn error of GABA metabolism. *Neuropediatrics*. 1998;29:14-22.
86. McKenna MC. Glutamate dehydrogenase in brain mitochondria: do lipid modifications and transient metabolon formation influence enzyme activity? *Neurochem Int*. 2011;59:525-533.
87. Denner LA, Weigel NL, Maxwell BL, Schrader WT, O'Malley BW. Regulation of progesterone receptor-mediated transcription by phosphorylation. *Science*. 1990;250:1740-1743.
88. Hemmings HC, Greengard P, Tung HYL, Cohen P. DARPP-32, a dopamine-regulated neuronal phosphoprotein, is a potent inhibitor of protein phosphatase-1. *Nature*. 1984;310:503-505.
89. Hokfelt T, Foster G, Schultzberg M, et al. DARPP-32 as a marker for D-1 dopaminoceptive cells in the rat brain: prenatal development and presence in glial elements (tanycytes) in the basal hypothalamus. *Adv Exp Med Biol*. 1988;235:65-82.
90. Meredith JM, Moffatt CA, Auger AP, Snyder GL, Greengard P, Blaustein JD. Mating-Related Stimulation Induces Phosphorylation of Dopamine- and Cyclic AMP Regulated Phosphoprotein-32 in Progestin Receptor-Containing Areas in the Female Rat Brain. *J Neuroscience*. 1998;18:10189-10195.
91. Holder MK, Veichweg SS, Mong JA. Methamphetamine-enhanced female sexual motivation is dependent on dopamine and progesterone signaling in the medial amygdala. *Horm Behav*. 2015;67:1-11.
92. Ghosh A, Greenberg M. Calcium signaling in neurons: molecular mechanisms and cellular consequences. *Science*. 1995;268:239-247.
93. Hardingham GE, Bading H. Synaptic versus extrasynaptic NMDA receptor signalling: implications for neurodegenerative disorders. *Nat Rev Neurosci*. 2010;11:682-696.
94. Schumacher M, Mattern C, Ghoumari A, et al. Revisiting the roles of progesterone and allopregnanolone in the nervous system: Resurgence of the progesterone receptors. *Prog Neurogibol*. 2013;113:6-39.
95. Luoma JI, Stern CM, Mermelstein PG. Progesterone inhibition of neuronal calcium signaling underlies aspects of progesterone-mediated neuroprotection. *J Steroid Biochem Mol Biol*. 2012;131:30-36.
96. Wu P, Zhao Y, Haidacher SJ, et al. Detection of structural and metabolic changes in traumatically injured hippocampus by quantitative differential proteomics. *J Neurotrauma*. 2013;30:775-788.
97. Chawla AR, Johnson DE, Zybura AS, Leeds BP, Nelson RM, Hudmon A. Constitutive regulation of the glutamate/aspartate transporter EAAT1 by Calcium-Calmodulin-Dependent Protein Kinase II. *J Neurochem*. 2017;140:421-434.
98. Hajnóczky G, Csordás G, Madesh M, Pacher P. The machinery of local Ca2+ signalling between sarco-endoplasmic reticulum and mitochondria. *J Physiol*. 2000;529:69-81.
99. Burté F, Carelli V, Chinnery PF, Yu-Wai-Man P. Disturbed mitochondrial dynamics and neurodegenerative disorders. *Nat Rev Neurol*. 2014;11:11.
100. Johri A, Beal MF. Mitochondrial dysfunction in neurodegenerative diseases. *J Pharmacol Exp Ther*. 2012;342:619-630.
101. Kemnitz JW, Gibber JR, Lindsay KA, Eisele SG. Effects of ovarian hormones on eating behaviors, body weight, and glucoregulation in rhesus monkeys. *Horm Behav*. 1989;23:235-250.
102. D'Eon T, Braun B. The roles of estrogen and progesterone in regulating carbohydrate and fat utilization at rest and during exercise. *J Womens Health Gend Based Med*. 2002;1:225-237.
103. Handgraaf S, Philippe J. The role of sexual hormones on the enteroinsular axis. *Endocr Rev*. 2019;40:1152-1162.
104. Boonyaratanakornkit V, Pateetin P. The role of ovarian sex steroids in metabolic homeostasis, obesity, and postmenopausal breast cancer: molecular mechanisms and therapeutic implications. *Biomed Res Int*. 2015;2015:140196.
105. O'Brien SN, Welter BH, Mantzke KA, Price TM. Identification of progesterone receptor in human subcutaneous adipose tissue. *J Clin Endocrinol Metab*. 1998;83:509-513.
106. Campbell SE, Febbraio MA. Effect of the ovarian hormones on GLUT4 expression and contraction-stimulated glucose uptake. *Am J Physiol Endocrinol Metab*. 2002;282:E1139-E1146.
107. Giles ED, Wellberg EA, Astling DP, et al. Obesity and overfeeding affecting both tumor and systemic metabolism activates the progesterone receptor to contribute to postmenopausal breast cancer. *Cancer Res*. 2012;72:6490-6501.
108. Beck CA, Weigel NL, Moyer ML, Nordeen SK, Edwards DP. The progesterone antagonist RU486 acquires agonist activity upon stimulation of cAMP signaling pathways. *Proc Natl Acad Sci USA*. 1993;90:4441-4445.
109. Mani SK, Blaustein JD, Allen JM, Law SW, O'Malley BW, Clark JH. Inhibition of rat sexual behavior by antisense oligonucleotides to the progesterone receptor. *Endocrinology*. 1994;135:1409-1414.
110. Tetel MJ, Beck CA, Ladtkow T, Christensen K, Weigel NL, Edwards DP. Functional properties and post-translational modification of steroid hormone receptors in the baculovirus expression system. In: Maramorosch K, Mitsuhashi J eds. *Invertebrate Cell Culture*. Enfield: Science Publishers Inc, 1997:201-210.
111. Diep CH, Knutson TP, Lange CA. Active FOXO1 Is a Key Determinant of Isoform-Specific Progesterone Receptor Transactivation and Senescence Programming. *Mol Cancer Res*. 2016;14:141-162.
112. Truong TH, Dwyer AR, Diep CH, Hu H, Hagen KM, Lange CA. Phosphorylated progesterone receptor isoforms mediate opposing stem cell and proliferative breast cancer cell fates. *Endocrinology*. 2018;160:430-446.
113. Forni PE, Taylor-Burds C, Melvin VS, Williams T, Wray S. Neural Crest and Ectodermal Cells Intermix in the Nasal Placode to Give Rise to GnRH-1 Neurons, Sensory Neurons, and Olfactory Ensheathing Cells. *J Neurosci*. 2011;31:6915-6927.
114. Lund C, Pulli K, Yellapragada V, et al. Development of Gonadotropin-Releasing Hormone-Secreting Neurons from Human Pluripotent Stem Cells. *Stem Cell Reports*. 2016;7:149-157.
115. Poliandri A, Miller D, Howard S, et al. Generation of kisspeptin-responsive GnRH neurons from human pluripotent stem cells. *Mol Cell Endocrinol*. 2017;447:12-22.

116. Casoni F, Malone SA, Belle M, et al. Development of the neurons controlling fertility in humans: new insights from 3D imaging and transparent fetal brains. *Development*. 2016;143:3969-3981.
117. Lund C, Yellapragada V, Vuoristo S, et al. Characterization of the human GnRH neuron developmental transcriptome using a GNRH1-TdTomato reporter line in human pluripotent stem cells. *Dis Model Mech*. 2020;13:dmm040105.
118. Willing J, Wagner CK. Progesterone Receptor Expression in the Developing Mesocortical Dopamine Pathway: Importance for Complex Cognitive Behavior in Adulthood. *Neuroendocrinology*. 2016;103:207-222.
119. MacLusky NJ, McEwen BS. Oestrogen modulates progestin receptor concentrations in some rat brain regions but not in others. *Nature*. 1978;274:276-278.

How to cite this article: Acharya KD, Nettles SA, Lichti CF, et al. Dopamine-induced interactions of female mouse hypothalamic proteins with progestin receptor-A in the absence of hormone. *J Neuroendocrinol*. 2020;e12904. https://doi.org/10.1111/jne.12904